PRODUCTION OF OXYGENATED FUEL ADDITIVE FROM GLYCEROL

A Thesis Submitted to the College of

Graduate Studies and Research

In Partial Fulfillment of the Requirements

For the Degree of Master of Science

In the Department of Chemical and Biological Engineering

University of Saskatchewan

Saskatoon

By

JEEVAN GARMILLA

PERMISSION TO USE

The author agrees to the terms that this thesis be made freely available to the libraries of the University of Saskatchewan for inspection. Furthermore, the author agrees that permission for the copying of this thesis in any manner, either in whole or part, for scholarly purposes be granted primarily by the professor(s) who supervised this thesis or in their absence by the Department Head of Chemical Engineering or the Dean of the College of Graduate Studies. Duplication, publication, or any use of this thesis, in part or in whole, for financial gain without prior written approval by the University of Saskatchewan is prohibited. It is also understood that due recognition shall be given to the author of this thesis and to the University of Saskatchewan for any use of the material in this thesis.

Request for permission to copy or make use of the material in this thesis in whole or in part should be addressed to:

The Head

Department of Chemical and Biological Engineering

College of Engineering

University of Saskatchewan

57 Campus Drive

Saskatoon SK Canada

S7N 5A9

ABSTRACT

Glycerol ethers have the potential to be used as additives with biodiesel as it can be easily blended and can improve fuel performance. It also facilitates easier passing of fuel through injector. Addition of glycerol ether increases the cetane number and improves the antiknocking property. Glycerol ethers are produced by reacting glycerol with tert-butanol (TBA).

To initiate the etherification reaction between two alcohols (glycerol and tert-butanol) on solid acid catalyst, acidity of catalyst is one of the primary requirement since the production of protonated molecules in the reaction mixture is crucial. In this work, acidic solid catalysts were developed by the impregnation of heteropolyacids (HPA, $H_3PW_{12}O_{40}$) on SBA-15 support. The SBA – 15 was prepared by hydrothermal method using P123 polymer, HCl, water and tetra ethyl ortho silicate (TEOS). Textural properties of the support were determined using N_2 – physisorption method and it was found that the surface area, pore volume and average pore diameters were 819 m^2/g, 1.14 cc/g and 5.02 nm, respectively. The pore volume can accommodate higher amount of HPA. HPA is acidic in nature and impregnation of HPA on support can develop the acidic functional groups. Generally, HPA is highly soluble in alcohol and addition of Cesium (Cs) can exchange the proton from HPA and inhibit the solubility by the formation of $Cs_xH_{3-x}PW_{12}O_{40}$. Three different catalyst samples were prepared by changing the Cesium (x) wt% (for x = 1.5, 2.2 and 2.9) on SBA-15 using incipient wetness method. These samples were dried at 120 ˚C for 2 hours and then calcined at 300 ˚C for 3 hours. The catalysts were characterized by N_2 physisorption, Fourier transform infrared spectroscopy (FTIR), X-ray diffraction (XRD), elemental analysis (inductively coupled plasma mass spectroscopy, ICP-MS), thermogravimetric/differential thermal analyzer (TG/DTA), scanning electron microscopy

(SEM), and temperature programmed desorption of ammonia (NH_3-TPD). The progressive reduction in textural properties of the support with HPA loading is identified in BET-Surface area. The enhancement of functional groups is indicated in FTIR. And also the change in crystalline nature is identified in XRD. The screened catalyst was used for etherification of glycerol.

Etherification of glycerol with TBA was performed in 100 ml autoclave and the product consists of mono, di and tri-tert butyl glycerol ethers along with some unreacted glycerol. The effects of various reaction parameters such as temperature, catalyst loading and molar ratio (glycerol/TBA) were studied to obtain an optimized condition for etherification of glycerol. Maximum conversion 76% of glycerol was achieved at the conditions of 120 °C, 1 MPa, 1:5 molar ratio (glycerol/TBA), 3% (w/v) catalyst loading and 800 rpm for 5 hours. The kinetic studies were performed and a mathematical model was developed using Langmuir-Hinshelwood mechanism. The reaction rate followed second order kinetics and the activation energy of 78 kJ/mol for the reaction signifies that the reaction was kinetically controlled.

Keywords: Fuel additive, Cesium (Cs), heteropolyacid (HPA), etherification, glycerol ether.

ACKNOWLEDGMENTS

I would first like to thank my supervisor, Dr. Ajay K. Dalai, for his mentorship, valued guidance and critical supervision throughout the planning, execution, and communication of my thesis work. I am extremely thankful to the time devoted by him to critically review and constructively criticize my written material. I would also like to thank the other two members of my advisory committee, Dr. Jafar Soltan and Dr. Hui Wang, for their contributions to my graduate studies and the time taken to review and critique my written materials.

Secondly, I would also like to thank Dr. Rajesh V. Sharma for his post-doctoral guidance, contribution and encouragement. Thanks also go to Mr. Richard Blondin, Mr. Dragan Cekic and Ms. Heli Eunike for their assistance in carrying out the laboratory work that contributed to my project. Special thanks go to Naveenji Arun for his friendship and couple of hours proof-reading my works. My thanks also go to the Natural Science and Engineering Research Council of Canada (NSERC) for their much-appreciated financial assistance. I also greatly appreciate the assistance from Geology and Mechanical Engineering Departments at University of Saskatchewan in catalyst characterizations.

Lastly, I would like to express my gratitude to my fellow students and members of catalysis and chemical reaction engineering laboratories, who were supportive during my graduate study in the University of Saskatchewan. Above all, I express my heartfelt thanks to my mother, father and brothers for their unconditional love and constant encouragement. Finally, I thank God Almighty for his blessings.

TABLE OF CONTENTS

LIST OF TABLES

LIST OF FIGURES

ABBREVIATIONS

T	Absolute temperature (˚C or K)
E	Activation energy (kJ/mol)
$\Delta H^{\ddagger}$	Activation enthalpy (kJ/mol)
$\Delta S^{\ddagger}$	Activation entropy (J/mol/K)
APR	Aqueous phase reforming
k_B	Boltzmann's constant ($1.381 * 10^{-23}$ J/K)
w_t	Catalyst loading (g)
C_{AS}	Concentration of A at catalyst surface (mol/l)
ρ_e	Density of the catalyst (kg/m^3)
DIB	Di-isobutylene
D & DTBGE	Di tert-butyl glycerol ether
D_e	Effective diffusivity (m^2/s)
η	Effectiveness factor
EPA	Environmental Protection Agency
ETBE	Ethyl tert-butyl ether
K	Equilibrium constant
k_0	Frequency factor (l/mol) min^{-1}
$\Delta G^{\ddagger}$	Gibb's free energy (kJ/mol)
G	Glycerol
C_{G0}	Initial concentrations of glycerol (mol/l)
C_{T0}	Initial concentrations of tert-butanol (mol/l)
IB	Isobutylene

LHSV	Liquid hourly space velocity (h^{-1})
MTBE	Methyl tert-butyl ether
M & MTBGE	Mono tert-butyl glycerol ether
P_T	Partial pressure of tert-butanol (bar)
P_W	Partial pressure of water (bar)
φ	Porosity
h	Plank constant ($6.626 * 10^{-34}$ J s)
k	Rate constant (l/mol) min^{-1}
R	Universal gas constant (8.314 J/mol/K)
STP	Standard temperature and pressure
S_a	Surface area (m^2/g)
TEL	Tetra ethyl lead
TAME	Tert-amyl methyl ether
TBA	Tert-butanol
Φ	Thiele modulus
ξ	Tortuosity
T & TTBGE	Tri tert-butyl glycerol ether
W	Water
WHSV	Weight hourly space velocity (h^{-1})

CHAPTER – 1

INTRODUCTION

Fossil fuels are considered as the major source of energy for today's world; these are extensively used by human beings to meet the energy requirements. Currently, fossil fuels are contributing 86% (36% oil, 27% coal and 23% natural gas) of the global energy demand (Maggio and Cacciola, 2012). Rapid depletion of fossil fuel and global warming by pollutant emissions are posing extra problems (Qurashi and Hussain, 2005). Presently, researchers are looking for new alternative energy resources and found that hydrogen, ethanol and biodiesel can complement the fossil fuels for energy (Quintana et al., 2011). The energy produced from alternative resources has considerable calorific value and are environmentally friendly (Quintana et al., 2011). Compared to fossil fuels, fuels from alternative energy sources have less greenhouse gas emissions (Song, 2006).

Diesel fuel is produced by fractional distillation of crude oil at 200 – 310°C and atmospheric pressure and it contains up to 20 carbon atoms per molecule (Satterfield, 1991). Diesel engine is also called as internal combustion or combustion-ignition engine in which fuel is compressed for ignition (Lapuerta et al., 2008). Gasoline engine is an internal combustion engine which has spark plug to ignite fuel-air mixture. Biodiesel is defined as a fuel comprising monoalkyl esters of long chain fatty acids derived from vegetable oil/animal fat and it should meet the ASTM standards of designation D6751 (Chang and Liu, 2010). Biodiesel has become an attractive fuel because of environmental benefits such as lower emission of carbon dioxide as compared to regular diesel (Dorado et al., 2003). Biodiesel consists of 10 wt% of oxygen, which improves the combustion efficiency (Oberweis and Al-Shemmeri, 2010). Biodiesel can be produced by transesterification of vegetable sources (soybean, sunflower, canola, cotton seed,

rapeseed and palm oil) and animal fats (Janaun and Ellis, 2010). Transesterification involves reaction of fat or vegetable oil with an alcohol to form an ester and glycerol. The global biodiesel market is estimated to reach 37 billion gallons (140 billion liters) by 2016 (www.dekeloil.com/nrg_biodiesel_global_market.html, 20th March, 2012). So it can produce approximately 4 billion gallons of crude glycerol. Currently, the production cost for biodiesel is higher than that of regular diesel due to higher cost of vegetable oils (Lee et al., 2011). To improve the biodiesel economy and the glycerol market, it is important to find potential applications for co-product glycerol. Glycerol can be used as source to produce various chemicals, viz. Syngas, hydrogen (Valliyappan et al., 2008), acrolein, formaldehyde, hydroxyacetone (Pathak 2005), acrylonitrile, propane diol, esters, ethers (Klepacova et al., 2007), surfactants (Guerrero-Perez et al., 2009), citric acid and lactic acid (Fan et al., 2010).

Diesel and gasoline are the major fuels in automobile sector; these are the derivatives of petroleum. These are burnt at high temperature in engine to produce heat. During burning, it releases harmful gases into atmosphere, causing pollution, global warming and acid rain (Quintana et al., 2011). Also, higher temperature combustion can affect the engine parts. To prevent the engine damage and also to protect the environment, it is necessary to add certain additives to these fuels. Tert-amyl methyl ether (TAME), methyl tert butyl ether (MTBE) and ethyl tert butyl ethers (ETBE) are the currently available fuel additives. Among these, MTBE usage is banned by EPA because it is highly soluble in water and also causes carcinogenic diseases in human beings. The remaining two additives (TAME and ETBE) are derivatives of non-renewable source such as petroleum. Since petroleum is depleting, now preference is to use biodiesel for diesel engines with slight modifications (Klepacova et al., 2003). Extensive research is in progress to produce additives from renewable sources such as glycerol, the fuel

additives produced from glycerol may have better engine performance and also reduce particulate matter emission (Frusteri et al., 2009). Glycerol ethers are used as fuel additives because they can be easily blended with diesel/biodiesel and can increase the fuel's cetane number (Lee et al., 2010). It enhances fuel combustion properties of diesel and decreases the cloud point of biodiesel (Klepacova et al., 2003).

The degree of unsaturation is one of the major disadvantages of biodiesel, and also it has cloud point of 0 °C. Lower cloud point is preferred for better performance of the fuel (diesel has -16 °C). Addition of glycerol ether can decrease the biodiesel cloud point (Klepacova et al., 2003). Glycerol ethers are easily soluble in biodiesel and can prevent polymerization by forming an oxygenated compound (Klepacova et al., 2007). It helps biodiesel to pass through the fuel injector and filter thus saving the maintenance cost. It also acts as antiknocking agent by increasing the cetane number and also increases the fuel efficiency by improving the combustion properties.

The Keggin structured heteropolyacid (HPA) is an inorganic acid, which is known as Bronsted acid and it is extensively used for esterification and transesterification reactions at both homogeneous and heterogeneous conditions (Zieba et al., 2009). The HPA are highly soluble in polar solvents (alcohol), to overcome such problem, insoluble HPA catalysts are prepared with exchanging protons by large cations like K^+, Cs^+ and NH_4^+ (Park et al., 2010). Among all alkali cations, Cs is recommended, because partial substitution of protons by Cs^+ (Eg: $Cs_xH_{3-x}PW_{12}O_{40}$) can enhance the number of acidic sites on surface and inhibit the solubility of HPA (Narasimharao et al., 2007). In the present work, insoluble $Cs_xH_{3-x}PW_{12}O_{40}$ is supported on

SBA-15 for the x (wt %) values of 1.5, 2.2 and 2.9 and these samples are named as Cat-1, Cat-2 and Cat-3, respectively.

1.1 Knowledge gap

Value added chemical production from glycerol can improve the biodiesel economy and glycerol market. Glycerol ethers are used as fuel additives; these can be easily blend in diesel/biodiesel and improve their combustion properties. Glycerol ethers are produced by reacting glycerol with an alcohol. Various glycerol ethers are reported in the literature, but there is limited literature available on tert-butyl glycerol ethers. Tert-butyl glycerol ethers are perfect replacement for petroleum derived fuel additives (MTBE, TAME and ETBE). Tert-butyl glycerol ethers are produced by reacting glycerol with tert-butanol.

Production of oxygenated fuel additive from glycerol is reported with commercial solid acid catalysts and no work is reported on activated biochar and SBA – 15 supported heteropolyacid catalysts.

1.2 Hypothesis

- Biochar and SBA – 15 supports can have high surface area (200 – 700 m^2/g), pore volume and pore diameters and hence can adsorb glycerol and TBA effectively due to low diffusional resistance.
- Glycerol etherification is an acid catalyzed reaction. The reaction between two alcohols (glycerol, tert-butanol) can be initiated with the formation of protonated molecules in the presence of acidic catalyst. These protonated molecules are highly reactive and react with OH group of an alcohol to form mono tert-butyl glycerol ether and water in the reaction mixture.

- Heteropolyacids (HPA), supported on porous materials, can be used as catalyst in esterification and transesterification reactions for the production of biodiesel. The catalytic activity is related to the amount of HPA presence on support.

1.3 Research objective

The objective of this work is to develop a catalyst for the production of oxygenated fuel additive from glycerol.

Phase I Synthesis of solid acid catalyst

This phase of the project was designed to synthesize the catalyst with impregnation of heteropolyacids on a porous support. Activated biochar and SBA-15 supports were synthesized and heteropolyacid (HPA) was loaded. The catalysts were calcined, characterized, screened and used for etherification of glycerol.

Preparation of supports and development of acidic sites

The activated biochar was prepared using chemical and steam activation methods. SBA-15 was prepared using P123 polymer, HCl, TEOS and water in hydrothermal method. Heteropolyacids are highly acidic in nature; impregnation on porous support can enhance the acidity. HPA are easily soluble in alcohols, so these are incorporated using wetness incipient method by dissolving in methanol.

Screening and characterization of the catalyst

The supports are screened for higher pore volume as they can accommodate more amount of HPA. The impregnation of HPA can develop acidic sites on the support. The catalyst samples were characterized for various techniques (see Table 1.1).

Table 1.1: Summary of catalyst characterization techniques

Technique	**Parameter**
BET surface area	Surface area, pore diameter and pore volume
Fourier transform infrared spectroscopy	Functional groups
Temperature programmed desorption of Ammonia	Acidity
X-Ray diffraction	Crystal structure
Scanning electron microscopy	Surface morphology
Inductively coupled plasma-mass spectroscopy	Elemental composition
Thermogravimetry/Differential thermal analyzer	Thermal stability
Malvern Mastersizer	Particle size distribution

Phase II Estimation of process parameters and kinetic study

During this phase of work, three different catalysts were prepared by changing the metal loading on support. The samples were calcined, screened and used as catalysts for etherification of glycerol with tert-butanol reaction. The effect of process parameters were examined and also the process was optimized for the maximum conversion of glycerol by varying temperature, catalyst loading and molar ratio (glycerol/TBA). Kinetic studies were performed to find the rate and order of the reaction. Kinetic equation was developed using Langmuir-Hinshelwood mechanism. Activation energy for etherification of glycerol reaction was determined by Arrhenius equation.

CHAPTER – 2

LITERATURE REVIEW

2.1 Production of biodiesel

Fossil fuels are considered as the primary energy source of the world and these were utilized since more than a century. Presently, world is consuming excess amount of fossil fuels and it is the right time for the replacement of fossil fuels by alternative fuels. Biodiesel, ethanol and hydrogen are the available alternative energy sources. According to Ma and Hanna (1999), biodiesel can be produced in four methods: direct use and blending, micro emulsion, thermal cracking (pyrolysis) and transesterification. Among all the reactions, transesterification reaction gives higher amount of pure biodiesel. Transesterification is the reaction of fat or vegetable oil with an alcohol to form biodiesel and glycerol (Dasari et al., 2005). One mol of glycerol is produced as co-product for every three moles of methyl esters (biodiesel), which is equivalent to approximately 10 wt% of the total product (Karinen and Krause, 2006). The obtained biodiesel is perfect replacement for regular diesel, as bio-based fuels have less impact on the engine parts (Demirbas, 2007). The utilization of biodiesel can decrease the hazardous pollutant emissions from engines and hence it is highly recommended for the future.

The global biodiesel market is estimated to reach 37 billion gallons by 2016 (www.dekeloil.com/nrg_biodiesel_global_market.html, 20th March, 2012). Approximately, four billion gallons of crude glycerol is produced. Production cost of biodiesel is higher than regular diesel due to the higher cost of raw materials. In order to decrease the biodiesel price, it is necessary to produce alternative value added chemicals from glycerol.

2.2 Utilization of glycerol

Glycerol (1, 2, 3-propane triol) is an oxygenated hydrocarbon (Valliyappan et al., 2008). The amount of glycerol production is directly proportional to the biodiesel production. Glycerol is used as emulsifying agent in pharmaceuticals, cosmetics, soaps and toothpastes (Behr et al., 2008). Glycerol has the potential to produce various chemicals such as syngas, hydrogen (Valliyappan et al., 2008), acrolein, acrylonitrile, formaldehyde (Pathak, 2005), propanediol, citric acid, lactic acid, esters, ethers (Klepacova et al., 2007), surfactants (Guerrero-Perez et al., 2009).

Hydrogen is an attractive energy source, which was derivative of fossil fuel. The production of hydrogen from alternative energy source such as glycerol can decrease the dependency on fossil fuels. Usage of glycerol for the production of valuable chemicals can increase glycerol market, which is economical for the biodiesel industries.

2.2.1 Production of hydrogen and synthesis gas

Hydrogen can be produced from the endothermic steam reforming of natural gas (Cheng et al., 2012). Generally, hydrogen is a potential raw material for various processes, such as production of ammonia, hydrotreating operations (Rapagna et al., 1998). Globally, production of hydrogen from alternative energy source is of great concern. Presently, glycerol is an alternative energy source, and it has the potential to produce hydrogen, synthesis gas (H_2 + CO) by pyrolysis, steam gasification and catalytic reforming (Valliyappan et al 2008).

Steam gasification of glycerol

One mol of glycerol ($C_3H_8O_3$) can effectively produce four moles of hydrogen. Valliyappan et al. (2008), conducted experiments on steam gasification of pure and crude glycerol in a fixed bed reactor with different packing materials (quartz and silicon carbide

particles). Commercial Ni/Al_2O_3 was used as catalyst. The steam gasification of the glycerol is represented in equation (2.1).

$$C_3H_8O_3 \rightarrow 3CO + 4H_2 \quad ----------(2.1)$$

In case of pure glycerol, the liquid hour space velocity (LHSV) and temperatures were maintained at 0.77 h^{-1} and 800 °C respectively. Addition of steam to glycerol increases the hydrogen production without altering the product composition. Increment of steam to glycerol weight ratio from 0:100 to 50:50 increased the amount of hydrogen production from 71 to 94 wt%.

For the steam gasification of crude glycerol, the liquid hourly space velocity (LHSV) and temperatures were maintained at 1.3 h^{-1} and 800 °C, respectively. Increment of steam to crude glycerol weight ratio from 25:75 to 50:50 increased the production of hydrogen from 78 to 91 wt%. The main reason for the less final conversion of crude glycerol in comparison to the pure glycerol in steam gasification is due to the presence of impurities (methanol, KOH and water) in crude glycerol.

Steam gasification can lead to some side reactions like steam reforming and water gas shift reactions and produce hydrocarbons (Valliyappan et al., 2008). For the production of concentrated hydrogen, reforming reaction was preferred (Behr et al., 2008). According to Cheng et al (2012), seven moles of hydrogen can be produced from one mole of glycerol (see reaction 2.2c).

Steam reforming of glycerol

Catalytic steam reforming of organic compounds is one of the methods used to produce hydrogen. Catalyst was mainly used to increase the reaction rate and also to increase the

selectivity of hydrogen. Steam reforming reaction of oxygenated organic compounds such as glycerol is an endothermic reaction and thus takes place at atmospheric pressure and temperature higher than 700 K and yields synthesis gas (Cheng et al., 2012). Because of the excess steam used in the process, carbon monoxide further undergoes water gas shift reaction to produce CO_2 and H_2 (Davda et al., 2005).

The individual steam reforming reaction is represented as decomposition of glycerol.

$$C_3H_8O_3 \rightarrow 3\ CO + 4H_2 \quad ----------(2.2\ a)$$

The amount of hydrogen production can be increased by water-gas shift reaction

$$3\ CO + 3H_2O \rightleftharpoons 3H_2 + 3CO_2 \quad ----------(2.2b)$$

The overall reaction is given in equation (2.2c)

$$C_3H_8O_3 + 3H_2O \rightarrow 7H_2 + 3CO_2 \quad ----------(2.2c)$$

Aqueous phase reforming (APR) of glycerol

Steam reforming of glycerol reaction requires atmospheric pressure and very high temperature. However, it has been noted that such reaction can occur efficiently at low temperature (500K) using high pressure (2-5 MPa) by aqueous phase reforming (APR) (Adhikari et al., 2008). APR reaction is similar to steam reforming (Ciftci et al., 2012). In this reaction, glycerol was kept in liquid phase and the reaction was tested at 225 °C, 2.9 MPa and these conditions were more favourable to water-gas shift reaction. The catalysts were prepared using Platinum (Pt) supported on Al_2O_3, SiO_2 and amorphous silica–aluminas with varying alumina content. The main products in gas phase were H_2, CO_2 and C1–C3 alkanes, liquid phase products were 1,2-propanediol, hydroxyacetone and C1–C3 monofunctional alcohols (Cifti et al., 2012).

Pyrolysis of glycerol

Pyrolysis of glycerol was studied in a packed bed reactor by Chaudhari and Bhakshi (2002) and they reported 70 mol% of synthesis gas production. Valliyappan et al. 2008, studied a wide range of reaction conditions by changing the carrier gas flow rate, temperature and packing material and their particle size. Finally, it was concluded that 72 wt% of glycerol got converted to 93.5 mol% of synthesis gas for the conditions of H_2/CO ratio of 1.05, 800 °C, 50 ml/min of carrier gas flow rate and 3-4 mm diameter of quartz packing material.

2.2.2 Production of acrolein, acrylic acid and acrylonitrile

Acrolein has wide range of applications. It is mainly used as micro biocide in oil wells, liquid hydrocarbon fuels, water treatment ponds, slimicide in the manufacture of paper and also used as major feed stock for 1, 3-propanediol. Acrolein can also be used to synthesize acrylic acid and its lower alkyl esters.

Watanabe et al., (2007) synthesized acrolein from glycerol in hot-compressed water using a batch and flow apparatus. It was reported that 74 mol % of acrolein yield and 81% of its selectivity was obtained with acid catalyst in supercritical condition (673 K, 34.5 MPa).

Acrolein also known as 2-propenal, acrylaldehyde or acrylic aldehyde, which is used as intermediate for the synthesis of many useful compounds as acrylic acid, acrylic acid esters, super absorber polymers and detergents (Guerrero-Perez et al., 2009). A sustainable and cost efficient dehydration of glycerol to acrolein could offer an alternative for the current commercial catalytic petrochemical process based on the reaction of propylene over a Bi/Mo-mixed oxide catalyst. In addition, direct synthesis of acrylonitrile and acrylic acid from glycerol is an attractive approach since both compounds are useful chemicals as raw materials for various synthetic resins, paints, fibers etc.

Pathak (2005) conducted a study on conversion of glycerol to liquid chemicals (acetaldehyde, acrolein, formaldehyde and hydroxyacetone) in a fixed bed reactor using HZSM-5, HY, silica-alumina and γ-alumina catalysts. The reaction conditions are maintained at 350 – 500 °C, 20 – 50 ml/min carrier gas flow rate and 5.4 – 21.6 h^{-1}weight hourly space velocity (WHSV). The complete conversion of glycerol was reported at 380 °C, 26 ml/min and 8.68 h^{-1} with silica-alumina and γ-alumina catalysts.

2.2.3 Fermentation

Glycerol fermentation process was used for the production of citric acid, lactic acid and 1, 3-propanediol. The synthesis processes were explained as follows.

Glycerol to citric acid

Citric acid is generally used as flavouring and preservative agent in food and beverages, especially soft drinks. Citric acid can be mixed with glycerol and used as plasticizer to increase the fluidity of the materials (plastics, concrete and wall board) (Tisserat et al., 2012). Citric acid can be produced by submerged fugal fermentation of sucrose or molasses medium using Aspergillus Niger (Fan et al., 2010). Many researches have produced industrial citric acid from inexpensive raw materials including crude glycerol. Rymowicz et al. (2006), examined the potential for citric acid biosynthesis by three acetate mutants of the yeast species Yarrowia lipolytica, including Strain K-1, Strain AWG-7, and Strain 1.31, under batch cultivation conditions on raw glycerol. The process is optimized for citric acid production by Yarrowia lipolytica in submerged fermentation using crude glycerol. Parameters like yeast extract, raw glycerol, and salt solution concentration were statistically analyzed using response surface methodology with Doehlert experimental design to evaluate the amount of citric acid produced.

The maximum citric acid concentration of 77.40g/l was obtained at the optimal conditions; yeast extracts 0.27g/l, raw glycerol 54.41 g/l, and salt solution concentration 13.70% (v/v).

Glycerol to lactic acid

The salts and esters of lactic acid have wide applications in the fields of food, cosmetic and pharmaceutical industries (Fan et al., 2010). The chemical modification of glycerol to lactic acid requires high temperature, high pressure and expensive catalyst. Hong et al., (2009) conducted experiments on microbial conversion of glycerol to lactic acid. Eight bacterial strains were investigated based on DNA sequences and physiological properties. It was found that the strain AC-521, a member of Escherichia coli, is the most suitable one for lactic acid production from glycerol. Optimal fermentation conditions were 42 °C, pH 6.5, and 0.85 min^{-1} (K_La). Maximum lactic acid concentration and glycerol consumption were achieved after 88 h of fed-batch fermentation.

Glycerol to 1, 3-propanediol

1, 3-propanediol is a simple organic chemical, which has high cost (42 $ per 100 g, Sigma Aldrich Canada, September 17, 2012) and low availability. It has wide range of applications in adhesives, laminates, power and UV-cured coatings, aliphatic polyesters, co-polymers and anti-freeze (Pachauri and He, 2006). 1, 3-propanediol can be produced from glycerol fermentation process using two step enzymatic reaction sequence (Guerrero-Perez et al., 2009). In the first step a glycerol dehydratase catalyzes the conversion of glycerol to 3-hydroxypropionaldehyde (3-HPA) and water. In the second step 3-HPA was reduced to 1, 3-propanediol by a NADH dependent 1, 3-propanediol dehydrogenase. The 1, 3-propanediol was

not metabolized further and it accumulates in the media. The activated carbon and zeolites were used as adsorbents for the separation of 1, 3-propanediol.

2.2.4 Esterification and Transesterification

Monoglycerides, polyglycerol esters and their derivatives are mostly used as emulsifiers in food, pharmaceutical and cosmetic industries (Guerrero-Perez et al., 2009). They were obtained by transesterification of glycerol with fatty methyl esters or with triglycerides (see Figure 2.1). Glycerol has three hydroxyl groups and hence, the product of esterification or transesterification reaction with acid or base catalysts was a mixture of mono, di and triglycerides, and unreacted glycerol. Direct esterification of glycerol with fatty acid requires strong base catalysts like KOH or $Ca(OH)_2$ (Singh and Fernando, 2009). In the presence of heterogeneous catalyst, (eg: Cs exchanged MCM-41), glycerol esters were obtained with 90% yield and 75% of monoglyceride (Barrault and Jerome, 2008). The basic catalysts KOH or $Ca(OH)_2$ have been used for the transesterification reaction. After reaction, they should be neutralized with phosphoric acid and the formed salts must be removed.

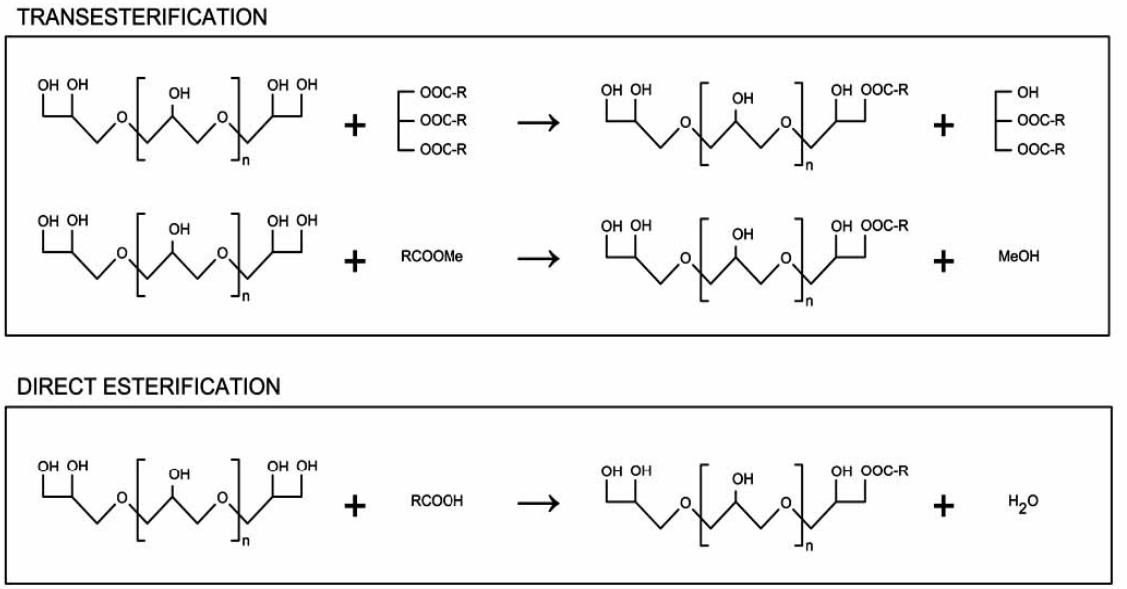

Figure 2.1: Esterification and transesterification of glycerol (Guerrero-Perez et al., 2009)

2.2.5 Etherification

Glycerol polymerizes at higher temperature, so it cannot be added directly to fuel (Noureddini et al., 1998). Glycerol is processed through selective etherification into glycerol ether, which is more valuable and suitable fuel additive for diesel/biodiesel (Gu Y et al., 2007). Addition of glycerol ether enhances the cetane number and also reduces the fumes and particulate matter, carbon monoxide emissions in the exhausts (Klepacova et al., 2003).

2.3 Importance of additive presence in fuel

The primary purpose of fuel additive is to enhance octane/cetane number by improving the anti knocking property of fuel. In early 1920's tetra ethyl lead (TEL) was used as an additive but it liberates lead into atmosphere which leads environmental and health problems by affecting the neural behaviour and also causing hypertension in adults (www.enotes.com/public-health-encyclopedia/fuel-additives March 10th, 2011). Finally, usage of lead was banned in 1995 (United States), and then methyl tert-butyl ether (MTBE) was used as an additive in place of TEL. MTBE reduces the carbon monoxide emission from fuel but it is highly soluble in water and can contaminate drinking water. MTBE is causing carcinogenic effects on animals. Finally it was also banned in 2001 by Environmental Protection Agency (EPA) at United States, now ethyl tert-butyl ether (ETBE) and tert-amyl methyl ether (TAME) are used as additives for diesel, but these are derivatives of petroleum. Petroleum is being depleted and now preference is to use biodiesel for diesel engines with slight modifications (Klepacova et al., 2003).

The usage of biodiesel has certain challenges. Biodiesel has polyunsaturated component and has tendency towards polymerization and forms a long chain molecule. It is difficult to pass the long chain molecule through fuel filter, so it accumulates and forms a gum like materials.

Cloud points of diesel and biodiesel were -16 ˚C and 0 ˚C. Lower cloud point was preferred for better performance of the fuel (Klepacova et al., 2003). In order to decrease the cloud point and also inhibit the polymerization additives are needed. Usually, methyl tert-butyl ether (MTBE), ethyl tert-butyl ether (ETBE) and tert-amyl methyl ether (TAME) are used as additives for diesel, these can be added in biodiesel too. These additives are produced from non-renewable fossil fuel resources like petroleum. The petroleum derived fuel additives are costly and cause environmental pollution, so there is extensive research in progress to produce fuel additives from alternative energy sources such as glycerol. Glycerol ethers are produced from etherification of glycerol with an alcohol. Addition of glycerol ether can reduce particulate matter and hazardous gas emissions from biodiesel (Klepacova et al., 2003), so it helps to prevent the environmental pollution.

2.4 Production of fuel additives from glycerol

Glycerol has three hydroxyl groups. When it reacts with an alcohol, it produces mono, di and tri glycerol ethers. The mono and di substituted glycerol ethers have two isomers. The reaction of glycerol with straight chain alcohol is given in Figure 2.2 (Gu et al., 2007).

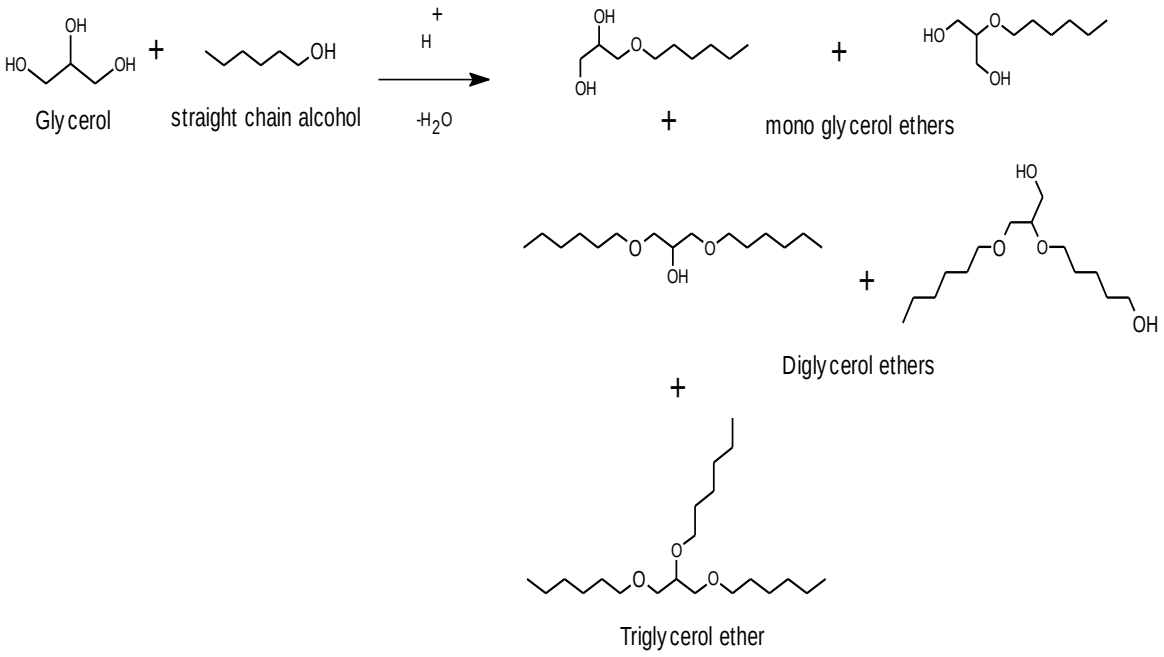

Figure 2.2: Reaction of glycerol with straight chain alcohol (Gu et al., 2007)

The required fuel additive can be selected based on the miscibility in biodiesel and also ability for cetane enhancement. In the above reaction, the alcohol has primary and secondary carbon atoms. In general, we need tert-carbon atom as it has higher magnitude for cetane number.

$$\text{Magnitude of cetane number: primary carbon} < \textit{secondary carbon} < \textit{tertiary carbon}$$

The straight chain alcohol in Figure 2.2 is replaced with isobutylene, which has tert-carbon atom. The produced ether is miscible in biodiesel and also decreases its cloud point (Klepacova et al., 2003).

2.4.1 Reaction of glycerol with isobutylene

Klepacova et al., 2007 studied on tert-butylation of glycerol with isobutylene using commercial solid acid catalysts and reported high glycerol conversion of 88% with zeolite H-T. Lee et al., 2010 studied similar reaction using Amberlyst-15 catalyst for the conditions of 50-100 ˚C and 20 MPa. Etherification of glycerol reaction was performed in stainless steel stirred autoclave with a mechanical stirrer, before the experiment glycerol and Amberlyst-15 catalyst were introduced into reactor and purged with nitrogen and then isobutylene was introduced (Lee et al., 2010).

The etherification of glycerol with isobutylene is shown in equations 2.3a, 2.3b and 2.3c below.

$$\text{Glycerol} + \text{Isobutylene (IB)} \rightleftharpoons \text{Mono tert} - \text{butyl glycerol ether (M)} - - - - \quad (2.3\ a)$$

$$\text{M} + \text{IB} \rightleftharpoons \text{Di tert} - \text{butyl glycerol ether (D)} - - - - - - - - - \quad (2.3\ b)$$

$$\text{D} + \text{IB} \rightleftharpoons \text{Tri tert} - \text{butyl glycerol ether} - - - - - - - - - - \quad (2.3\ c)$$

Simultaneously, two side reactions take place to form tert-butyl alcohol (TBA) and oligomers of isobutylene (see equations 2.3d and 2.3e).

$$\text{IB} + \text{H}_2\text{O} \rightleftharpoons \text{Tert} - \text{butyl alcohol} - - - - - - - - - - - - - \quad (2.3\ d)$$

$$2\text{IB} \rightarrow \text{Di} - \text{isobutylene} - - - - - - - - - - - - - - - - - - - \quad (2.3\ e)$$

Di-isobutylene (DIB) formation and glycerol conversion were observed within two hours of reaction time in the presence of one mm Amberlyst-15 beads. After five hours of reaction, significant amount of mono tert-butyl glycerol ether (MTBGE) was produced, and then the rate

of etherification was accelerated due to the solvent effect. MTBGE is a very good solvent for glycerol and isobutylene, and facilitates the transport of reactants within the pores. The more MTBGE is produced, the higher is the reaction rate, and after 7 hours of reaction almost all glycerol is converted to di-ether (DTBGE) and tri-ether (TTBGE). The distribution of products depends on the ratio of isobutylene to glycerol, mostly tri and di ethers were formed at high IB/G ratio, mono and di ethers were formed at low IB/G ratio. It is difficult to obtain single ether at the high level of glycerol conversion.

The isobutylene is in gas phase and glycerol is in liquid phase at room temperature. For combining these two phases to induce the etherification reaction, high pressure (20 MPa) is required. With high pressure, isobutylene oligomerizes to form di-isobutylene (DIB). When DIB forms, there is a shortage of isobutylene (IB) for etherification (Lee et al., 2010). It is difficult to stop the oligomerization of IB. So in this reaction IB was replaced by tert-butyl alcohol (TBA).

2.4.2 Reaction of glycerol with tert-butanol

Glycerol ethers are produced by reacting glycerol with an alcohol. Highly acidic solid acid catalyst is required to initiate the reaction between two alcohols (Gu et al., 2008). Da Silva et al. (2009) reported that in the presence of excess alcohol mono ether is produced which undergoes self-etherification to form di and tri ethers of glycerol. The reaction between glycerol and tert-butyl alcohol (TBA) at 1:4 molar ratio can produce mono, di and tri butyl glycerol ethers (Klepacova et al., 2003). According Fursteri et al. 2009, the reaction of glycerol and TBA can producue five different alkyl glycerol ethers such as mono (1 or 3) tert-butyl glycerol ether, di

(1,1 or 1, 2) tert-butyl glycerol ether and tri tert-butyl glycerol ether (see Figure 1). Gu et al., 2008 reported that glycerol and TBA at 1:1 molar ratio doesn't undergo self-etherification.

The etherification reaction of glycerol with tert-butanol (TBA) was studied by Frusteri et al., (2009) using a stainless steel jacketed-batch reactor with a magnetic stirrer. Initially the weighed amount of glycerol and dry catalyst were loaded into the reactor and heated up to desired reaction temperature (in 10 min). Before the addition of tert-butanol, the reactor was purged with nitrogen to remove the air; then, tert-butanol was injected into the reactor by a syringe. At the end of the experiment, the reactor was cooled down to 25 ˚C by an ice bath until the vapour pressure of the mixture equalled to the atmospheric pressure. The mixture was collected by opening the auto clave without any solidification of TBA (melting point is 23-26 ˚C) on the reactor walls. The liquid reaction mixture composition was analyzed by a gas chromatograph and the product distribution is shown in Figure 2.3.

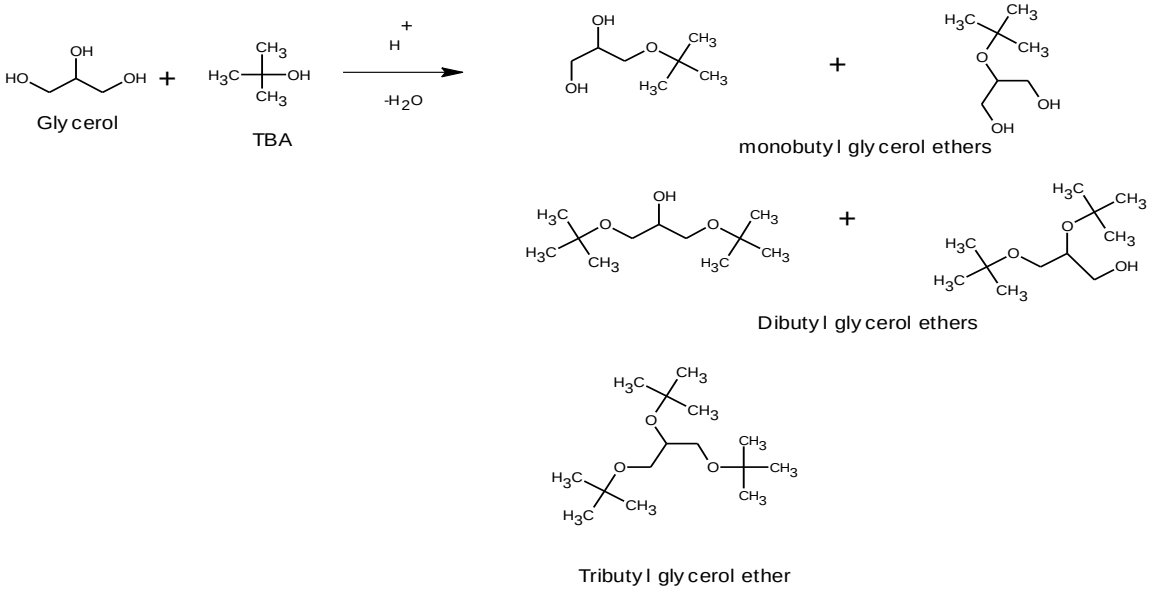

Figure 2.3: Etherification of glycerol with tert-butyl alcohol (TBA) (Frusteri et al., 2007)

Glycerol conversion linearly increased with increase in temperature and catalyst/glycerol weight ratio. There was no product observed without any catalyst and a significant glycerol ether formation could be observed as the amount of catalyst increased. The highest yield to ethers of glycerol (DBGE + TBGE) was obtained with an amount of catalyst equivalent to 7.5 wt% with respect to the mass of glycerol.

2.5 Mechanism of glycerol etherification

When glycerol reacts with tert-butanol (TBA), it produces ether and water (see Figure 2.4). In the presence of acidic and porous catalyst, the adsorbed TBA on the catalyst surface can release the proton (H^+) into the reaction mixture. These protonated molecules are highly reactive and they react with glycerol to form mono tert-butyl glycerol ether and water. The mono tert-butyl glycerol is adsorbed on the catalyst surface and undergoes further etherification to produce di and tri tert-butyl glycerol ethers (see Figure 2.4).

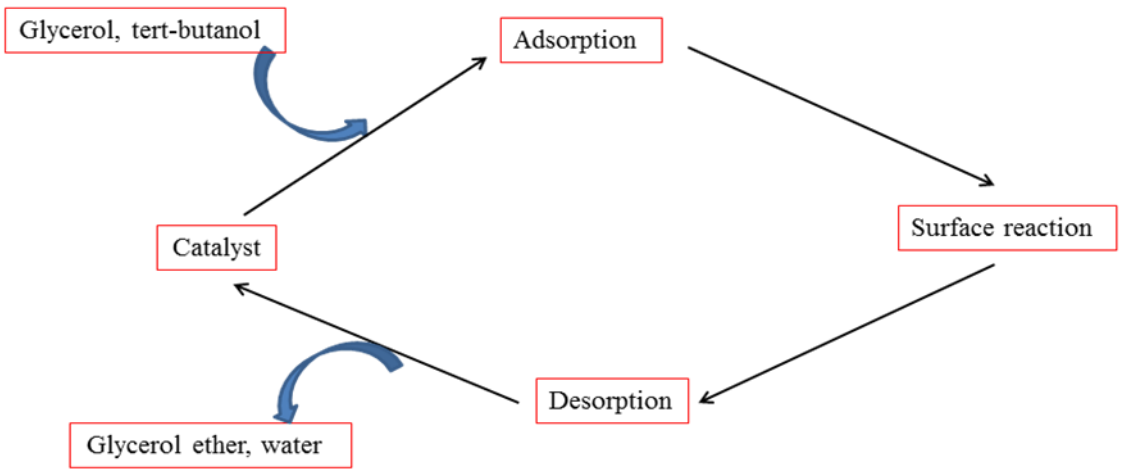

Figure 2.4: Mechanism of glycerol etherification (Yadav et al., 2011)

Glycerol etherification reaction follows Langmuir-Hinshelwood kinetics, and it happens in 3 steps (shown in Figure 2.4 as adsorption, surface reaction and desorption).

Step 1: Adsorption of glycerol and an alcohol on catalyst surface

Glycerol is highly viscous compound, so higher surface area of the catalyst is required for adsorption. Glycerol (A) and an alcohol (B) get adsorbed on the active site of the catalyst surface (S) (see equations 2.5a and 2.5b).

$$A + S \rightleftharpoons A.S \quad (2.5\ a)$$

$$B + S \rightleftharpoons B.S \quad (2.5\ b)$$

Step 2: Surface reaction of adsorbed glycerol and alcohol

Adsorbed glycerol (A.S) and alcohol (B.S) undergo surface reaction and form mono glycerol ether (C.S), water (D.S) as product and co-product (see equation 2.5c). To induce the surface reaction among two adsorbed molecules Bronsted acidity is required. Therefore, acidity of the catalyst is responsible for the surface reaction. Higher pore volume of the catalyst is required to avoid diffusional resistance.

$$A.S + B.S \rightleftharpoons C.S + D.S \quad (2.5\ c)$$

Step 3: Desorption of produced mono glycerol ether and water

Mono glycerol ether and water produced by surface reaction is held on the catalyst surface. These products desorb and detach from the surface of catalyst then the remaining active site (S) is again available for further etherification (see equations 2.5d and 2.5e).

$$C.S \rightleftharpoons C + S \quad \text{(2.5 d)}$$

$$D.S \rightleftharpoons D + S \quad \text{(2.5 e)}$$

The active sites of the catalyst adsorb fresh glycerol and also the product (mono ether), undergo further etherification and produces di and tri glycerol ethers. So the extent of bulk ethers adsorption depends upon the porosity of the catalyst. Highly porous catalysts can adsorb mono ethers and which undergo for further etherification.

The catalyst plays an important role in extent of etherification. For more conversion of glycerol, catalyst is required with acidity and higher pore volume.

2.6 Influence of acidity and pore volume on glycerol etherification reaction

According to Da silva et al. (2009), acidity plays an important role in etherification. Different types of Amberlyst catalysts (Amberlyst-15, Amberlyst-35 and Amberlyst-36 with acidity ranges of 4.2-5.6 mmol/g showed good performance than other catalysts due to their higher acidic nature. The Bronsted acidic sites can release proton (H^+) into the reaction mixture, which is highly reactive and it reacts with OH group of alcohol and forms water. The protonated alcohol reacts with glycerol and forms mono glycerol ether. Therefore, the extent of mono ether formation depends on the acidity of the catalyst, and then the series of etherification reactions

depend on the available active sites of the catalyst (Hermida et al., 2011). The usage of commercial catalysts was limited due to its surface area (53 m^2/g) and lack of thermal stability. Heteropolyacids are highly acidic in nature and thermally stable (Yadav and George, 2008), so the incorporation of these can develop the acidic sites on the support. So higher pore volume is preferred to accommodate more amount of heteropolyacids.

CHAPTER – 3

EXPERIMENTAL METHOD

3.1 Synthesis of activated biochar

Biomass mainly consists of C, H, N, O, S, moisture and volatile materials, these have low pore volume and pore diameter, thermal treatment on biomass removes moisture and volatiles, the remaining biochar shows different textural properties than initial material due to change in pore structure and surface area (Lehmann et al., 2011). The change in pore properties enhances the adsorption capacity, so this biochar is activated and used as adsorbent in chemical industries to removes organic compounds from air and water (Ni et al., 2011).

3.1.1 Preparation of biochar

Biochar was produced by fast and slow pyrolysis. In fast pyrolysis, biomass was heated rapidly for 5-10 seconds at 400-550 °C. In slow pyrolysis, biomass was heated for at least 30 minutes to several hours at 400-600 °C (Wright et al., 2008). During pyrolysis, biomass is converted into three products.

1. Solid char is formed and it has wide range of applications. It is used as catalyst in chemical reactions and also used to separate organic content from municipal waste water.
2. Liquid product is formed and it is called as bio-oil or pyrolysis oil or bio-crude.
3. A non-condensable gas product is formed which consists of carbon monoxide, carbon dioxide, methane, higher hydrocarbons and synthesis gas.

Ringer et al., (2006) reported that slow pyrolysis produces about 30% bio oil, 35% of biochar and 35% of syn gas. Wright et al., (2008) reported that fast pyrolysis yields about 70% bio oil,

15% biochar and 13% syn gas. Maximum amount of biochar can be produced from slow pyrolysis of biomass.

Biochar structure can be determined by X-ray diffraction and it is mostly amorphous in nature, but contains some local crystalline structure of highly conjugated aromatic compounds (Qadeer et al., 1994). Pyrolysis of biomass enlarges the crystallites and gives a proper shape. Lua et al., (2004) reported that increasing the pyrolysis temperature from 250 to 500 °C increases the BET surface area due to the increasing evolution of volatiles; this enhances the pore structure of biochar. Physical structure of the biochar can be altered by chemical and steam activation methods.

3.1.2 Activation

In the present work, biochar was obtained from Dynamotive, which was treated in chemical and steam activation methods. In chemical activation method, volatile material was removed to create voids, and then it was treated with fresh steam in steam activation method to increase the size of voids.

3.1.2.1 Chemical activation

Chemical activation method was carried out in a single step with the combination of carbonization and activation. The biochar was treated with nitric acid in a round bottom flask at 120 °C for 2 hours. The flask was connected to an open condenser where cooling water was circulated through the outside walls. 10 g of biochar material was treated with 120 g of nitric acid (70 wt %). The partial removal of carbon in the form of CO_2 can create pores in biochar. The acid treated biochar was separated from the acidic solution through filtration; the pH of

treated biochar was adjusted to neutral with continuous water washing (Zhang et al., 2004). Only four grams of biochar was recovered after the chemical activation for two hours. Very less amount of biochar yield was observed for more than two hours of chemical treatment.

3.1.2.2 Steam activation

The acid treated biochar is then treated with pure steam for steam activation. 8 g of acid treated biochar is taken in inconel tubular reactor (outer diameter 2.54 cm, inner diameter 2.2 cm, length 87 cm). The conditions are maintained at 723 °C with constant flow of steam (7 ml/h) along with N_2 (138 STP/min) (Azargohar and Dalai, 2008). At these conditions biochar releases the volatile material with partial devolatilization and the process enhances the crystalline carbon formation (Alaya et al., 2000). The passage of pure steam enlarges the size of existing pores (Rodriguez-Reinoso et al., 1992). 3.5 g of steam activated biochar was obtained at 1.4 hours of operation. The steam activated biochar is usually used for adsorption of organic compounds from industrial/municipal water. The adsorptive properties of biochar depend upon activation time and quantity of steam used for activation.

3.2 Synthesis of SBA-15

Mesoporous SBA-15 was synthesized from P123 polymer, water, HCl and tetra-ethyl ortho silicate (TEOS) using hydrothermal method (Vinu et al., 2006) (see Figure 3.1). Briefly, 24 g of P123 was added to 946 ml water, stirred at 40 °C for two hours, 126 g of HCl was added slowly by maintaining at 40 °C for four hours. After complete dissolution of P123 in HCl, silica source (TEOS) was added and stirred for 24 h at 40 °C. The mixture was transferred to a Teflon bottle and kept for aging at 120 °C for 24 h. The product was cooled, filtered and washed until

the pH becomes neutral, dried at 120 °C and finally calcined at 550 °C for five hours to obtain mesoporous SBA-15.

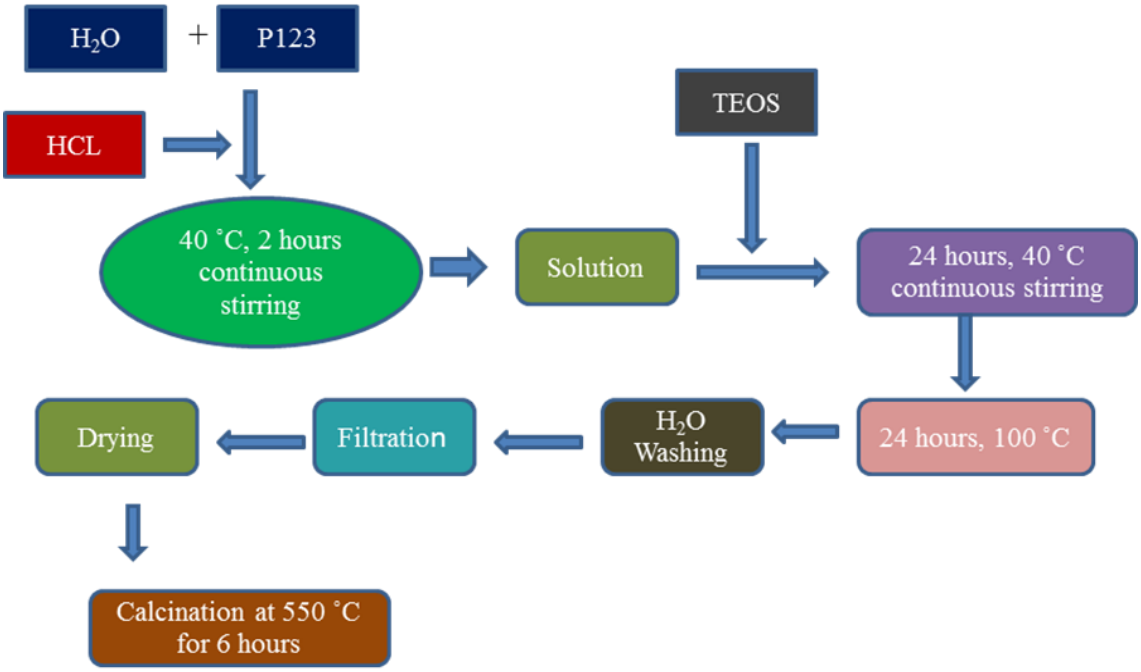

Figure 3.1: Synthesis of SBA-15 using hydrothermal method

3.3 Screening of the support

Highly porous and acidic catalyst was preferred for glycerol etherification. Heteropolyacids (HPA, $H_3PW_{12}O_{40}$) were highly acidic in nature; higher pore volume can help to accommodate more amount of HPA, which can increase acidity (Bokade and Yadav, 2012). The supports were screened for higher pore volume. The crude biochar doesn't have significant pore volume, so it was treated in different activation methods to enhance the pore volume. The steam activated biochar has maximum pore volume of 0.08 cc/g, but it was comparatively less to

mesoporous SBA-15, which has the pore volume of 1.14 cc/g (see Table 4.1). Therefore, SBA-15 was screened and HPA were incorporated by wetness incipient method.

3.4 Impregnation of heteropolyacids on support

HPA are acidic in nature, the incorporation of HPA on SBA-15 can develop the acidic sites, but these are soluble in alcohol. In glycerol etherification reaction, glycerol and tert-butanol are alcohols, so the HPA can form a homogeneous mixture. To overcome such problems, the insoluble HPA are prepared with an exchange of proton by large cations like K^+, Cs^+ and NH_4^+ (Park et al., 2010). Among all alkali cations, Cs is recommended, because partial substitution of protons by Cs^+ (Eg: $Cs_xH_{3-x}PW_{12}O_{40}$) can enhance the number of acidic sites on surface and inhibit the solubility of HPA (Narasimharao et al., 2007). The $Cs_xH_{3-x}PW_{12}O_{40}$ supported on SBA-15 samples are synthesized for x = 1.5, 2.2 and 2.9 using wet incipient impregnation method (Yadav and George 2008), these samples are named as Cat-1, Cat-2 and Cat-3 respectively (see Figure 3.2). The Cesium Chloride (CsCl) is used as Cesium source. Firstly, the measured amount of CsCl is dissolved in methanol, and its volume is maintained equal to the pore volume of the support. This solution is slowly added to SBA-15, mixed and dried at 120 °C for 2 h. Then, the dodeca tungstophosphoric acid (DTP) is dissolved in methanol and its volume is also maintained equal to the pore volume of the support. This solution is added to the dried sample, mixed and dried at 120 °C for 4 h. The proton exchange from DTP helps to form $Cs_xH_{3-x}PW_{12}O_{40}$ and HCl. In order to remove HCl, the sample is calcined at 300 °C for 3 h (Bokade and Yadav, 2012). The choice of methanol as a solvent for deposition of DTP structure on SBA-15 is explained well in literature (Soni et al., 2011).

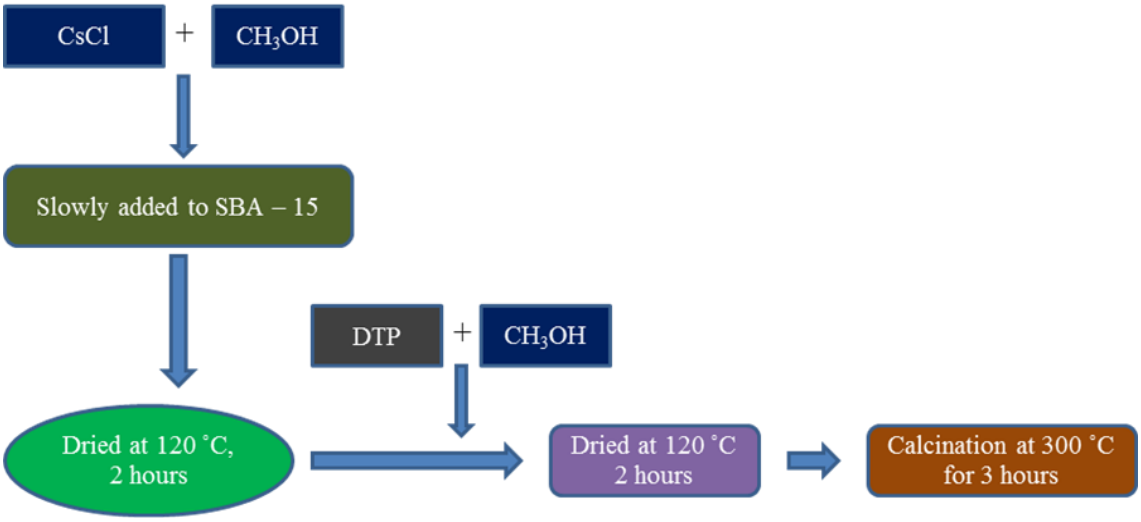

Figure 3.2: Impregnation of heteropolyacid on support

3.5 Characterization

The BET surface area, pore volume and average pore diameter of the support and catalysts are measured using Micromeritics ASAP 2000 instrument with N_2 physisorption at -196 °C. Initially, the dried sample (0.2 g) is degassed in vacuum at 200 ˚C for 2 h to remove moisture. The BET surface area is calculated based on the adsorption data in the partial pressure range (P/P_0) from 0.05 to 0.99. The pore volume and average pore diameters are calculated using BJH method by assuming that the adsorption on external surface is negligible.

The impregnation of heteropolyacids on SBA-15 can help to develop the functional groups which are analyzed by Fourier Transform Infrared (FTIR) Spectroscopy. Samples were dried, mixed with KBr in 1:19 weight ratio and ground into fine powder, 7 tonnes of load is applied to make a soft and thin pellet. This pellet is scanned with IR in wave number range of 400 – 4000 cm^{-1}. The percentage transmission is recorded and plotted against wave number.

The heteropolyacids are in crystalline form and SBA–15 is in amorphous form. The impregnation of heteropolyacids on SBA-15 can change the phase composition, which is determined by X-ray diffraction (XRD). The analysis is carried out with a fine powder of sample in Bruker Advance II series instrument equipped with Copper radiation at voltage of 20 kV and a current of 20 mA. Each sample is scanned for low angle (0.5 – 10°) and wide angle (10 – 80°) separately.

The thermal stability of the catalyst is determined using PerkinElmer thermo gravimetric differential thermal analyzer with an argon flow of 90 ml/min. The dried sample is analyzed from 27 to 500 °C with 10 °C /min ramp rate, kept at 500 °C for 10 minutes, and then cooled to room temperature. The change in weight with temperature is recorded.

The elemental compositions of cesium (Cs) and Tungsten (W) metals over the support were identified using Inductively Coupled Plasma Mass Spectroscopy (ICP-MS) instrument. The catalyst sample is dissolved in HF acid at 100 – 150 °C for 3 days. After cooling, samples are further dissolved in concentrated HNO_3 for complete dissolution of metals. The amount of metal content is determined using a mass spectrometer.

The morphology of support and HPA incorporated catalyst samples are analyzed with JEOL 840A scanning electron microscope. The images were acquired with a working distance of 15 mm for the low magnification shots and 8 mm at high magnification. The electron gun was operated at an accelerator voltage of 20 keV.

The particle size distribution of the catalyst sample is identified by Malvern Mastersizer S Long Bench particle size analyzer. It determines the particle size using optical techniques, 300 RF lens is used, which has the particle size range of 0.05 – 800 μm.

The total acidity of the catalyst was determined by the ammonia temperature programmed desorption using a Micromeritics Auto Chem 2920 (USA) instrument. The 0.1 g of catalyst sample was loaded in a quartz cell and pre-heated to 120°C for 10 min. and heated again to 350º C for 30 min. with helium flow of 30 ml/min. Then the cell was cooled down to 50 °C and ammonia was allowed to adsorb by exposing 10 % ammonia in He gas for 1 h. The excess ammonia was removed with He flush for 30 min. Then the adsorbed ammonia was desorbed by heating the cell from 50 °C to 350 °C with heating rate of 30 °C /min with 30 ml/min flow of He. The desorbed ammonia was detected by TCD.

3.6 Reaction set up and installation

The 100 ml volume autoclave has taken from Parr instrumentation company (USA), which is heated using a jacketed vessel at the outer side. Thermocouple and pressure gauge are mounted on top to measure the inside temperature and pressure of the reactor. The reactor has a gas inlet valve on one side and outlet valve for other side. A motor is installed over head of the reactor, which connected to an impeller with a shaft to agitate the reaction mixture.

The reactor setup and its internal structure are shown in Figures 3.3 and 3.4 respectively.

Figure 3.3: Reactor set up

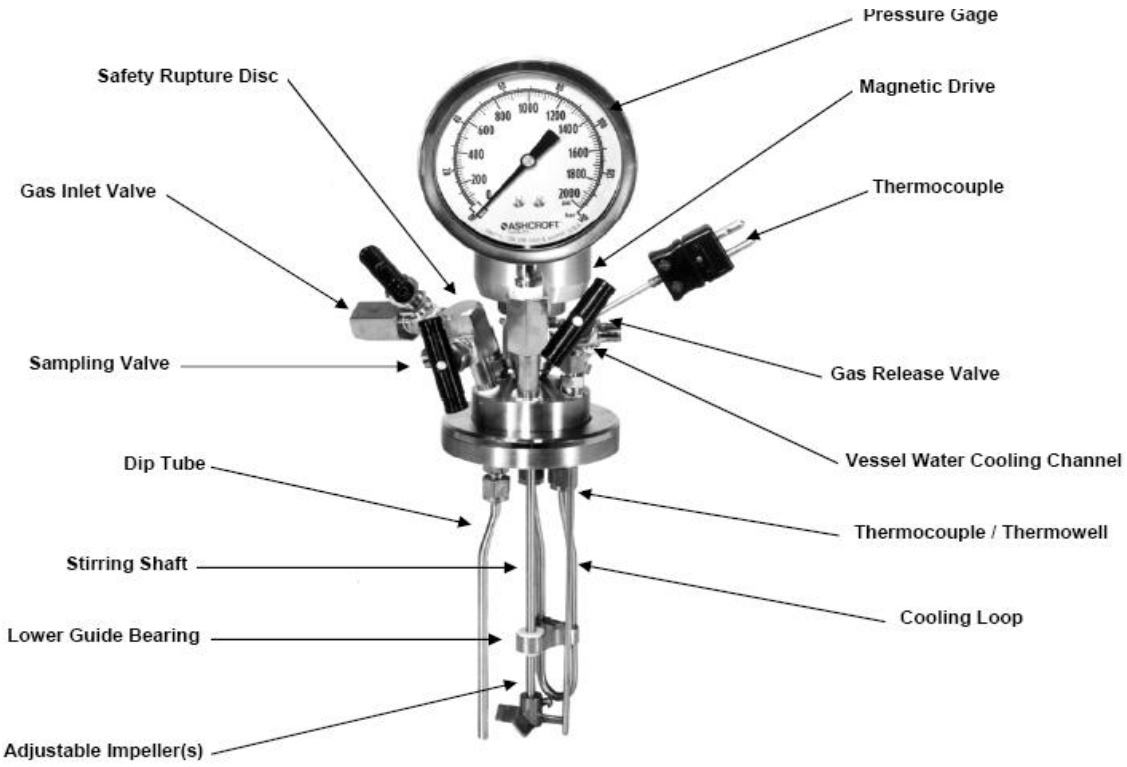

Figure 3.4: Parr reactor with valves (4560 mini bench top reactors, Parr Instrumentation Company)

Initially, weighed amount of glycerol, dry catalyst and tert-butanol are taken in an autoclave, heated with a high watt density heater up to the desired temperature. Inert atmosphere was maintained with 1 MPa of N_2. Then, the stirrer is turned on and maintained at 800 rpm. The reaction mixture was collected every 1 hour interval through sampling valve (see Figure 3.4). After 5 hours, the stirrer was stopped, reactor was cooled down to room temperature and the catalyst was separated from the reaction mixture through filtration. The filtered reaction mixture was transferred into 2 ml glass vial and diluted with propanol, analysed in GC with installation of stabilwax column. Then the results obtained from GC are compared with model compounds to analyze the peaks. The reaction was repeated and the glycerol conversion and mono, di and tri tert-butyl glycerol ether formations were determined. Finally, the reaction parameters were studied for higher conversion of glycerol.

3.7 Catalyst activity

Etherification of glycerol reaction was performed in a 100 ml autoclave, equipped with a mechanical stirrer, electrically heated up to the desired temperature and the inert atmosphere was maintained with N_2. The screening studies were performed with Cat-1, Cat-2 and Cat-3 at 110 °C and 120 °C by maintaining the process conditions at 1 MPa, 1:4 molar ratio (glycerol/TBA), 2.5% (w/v) catalyst loading and 800 rpm for 4 hours. The process was studied with the screened catalyst for the effects of temperature, catalyst loading and molar ratio (glycerol/TBA).

3.8 Product analysis

After etherification reaction, the samples were collected using sample outlet valve for every hour by stopping the mixing. The samples were centrifuged, filtered, transferred into 2 ml glass vial, diluted with propanol and analyzed in GC using Hewlett Packard 5890 series II equipment with installation of stabil wax column (length 30 m, internal diameter 0.25 mm and width 0.1 μ m). Glycerol ethers are highly polar compounds, so wax column was preferred in GC for its analysis (Klepacova et al., 2003). Helium was used as carrier gas; air and hydrogen were used to ignite the FID. The program was started at 40 °C, heated up to 240 °C with 20 °C/min ramp rate and kept for 5 minutes of holding. The injector and detector temperatures were maintained at 280 °C.

In typical analysis, 130 μl of reaction mixture was taken in 2 ml vial, diluted with 1200 μl propanol and 20 μl of n-hexanol was added as external standard to decrease the sample injection errors. 1 μl of sample was taken from vial, the oven was cooled down to 40 °C then the sample was injected. The analysis took 17 minutes to elute the compounds, the peak area from GC corresponds to the concentration of each component present in the mixture. The conversion of glycerol was calculated by the ratio of moles of glycerol converted to the total moles of glycerol. The performance of the catalyst is evaluated based the selectivity for mono, di or tri tert-butyl glycerol ether and its yields. The selectivity and yields are defined by the following equations (Xiao et al., 2011)

$$\text{Conversion } (\%) = \frac{\text{moles of glycerol converted}}{\text{total moles of glycerol}} * 100$$

$$\text{Selectivity of mono, di or tri tert} - \text{butyl glycerol ether } (\%) = \frac{\text{moles of glycerol converted to mono, di or tri ether)}}{\text{total moles of glycerol converted}} * 100$$

$$\text{Yield } (\%) = \frac{\text{Conversion } (\%) * \text{ Selectivity } (\%)}{100}$$

CHAPTER – 4

RESULTS AND DISCUSSIONS

This chapter consists of results for characterization of the catalyst samples, screening of the catalysts with various HPA loadings, optimization of process parameters (temperature, catalyst loading, molar ratio (glycerol/TBA)) and kinetic study. Also, the effect of transport limitations are studied.

4.1 Characterization

The catalyst samples were characterized with BET surface area, FTIR, XRD, TG/DTA, ICP-MS, SEM, NH_3-TPD and particle size distribution.

4.1.1 Measurement of textural properties

The textural properties of support and HPA loaded catalysts were analyzed using BET surface area method. The analysis was carried out twice to check for reproducibility and the average values are reported in Table 4.1.

The SBA-15 has a surface area of 819 m^2/g and average pore diameter of 5.02 nm indicating that it is a mesoporous material (Satterfield, 1991). The BET surface area and pore volumes of the heteropolyacid loaded catalysts were less compared to those of pure support. The increment of Cesium loading from 1.5 (Cat-1) to 2.9 % (Cat-3) decreased the surface area and pore volume from 781 to 702 m^2/g and 1.09 to 0.94 cc/g, respectively. The decrease in surface area and pore volume was due to the formation of $Cs_xH_{3-x}PW_{12}O_{40}$ on surface and also in the pores of SBA-15 (Kraleva et al., 2011). The average pore diameter for Cat-1 (4.98 nm) was comparatively higher than Cat-2 (4.92

nm) and Cat-3 (4.85 nm) and it is due to the lesser blockage of pore opening in Cat-1 with HPA.

Table 4.1: Textural property of different catalysts

Sample	**BET surface area (m^2/g)**	**Pore volume (cc/g)**	**Avg. pore diameter (nm)**
HNO_3 treated biochar	4	0.05	4.02
Steam activated biochar	369	0.08	3.52
SBA-15	819	1.14	5.02
Cat-1	781	1.09	4.98
Cat-2	707	0.99	4.92
Cat-3	702	0.94	4.85

4.1.2 Functional group identification using Fourier Transform Infrared Spectroscopy

The FTIR spectra of HPA and supported catalysts were given in Figure 4.1. The sharp peaks in analysis of HPA at wave numbers of 1077, 981, 885 cm^{-1} indicate P-O, W-O and W-O-W bond stretching (Bokade and Yadav 2012) and peaks at 591 and 515cm^{-1} show terminal W-O-W asymmetric vibrations associated with Keggin ion (Yadav et al., 2011). The proton exchange with Cesium (Cs) helps to form Keggin structure of HPA on SBA-15. After the impregnation of HPA on SBA-15, one peak was observed at 885 cm^{-1} for Cat-2 and three peaks were observed at 981, 885 and 591 cm^{-1} for Cat-3. The intensity of the bond stretching at 885 cm^{-1} was higher for Cat-3 due to the increase in HPA loading. Therefore, at higher amount of loading (for X = 2.2 and 2.9), the Keggin structure formed was stable and for lower amounts of loading (X=1.5), the structure was unstable and no peak was observed for Cat-1 (see Figure 4.1).

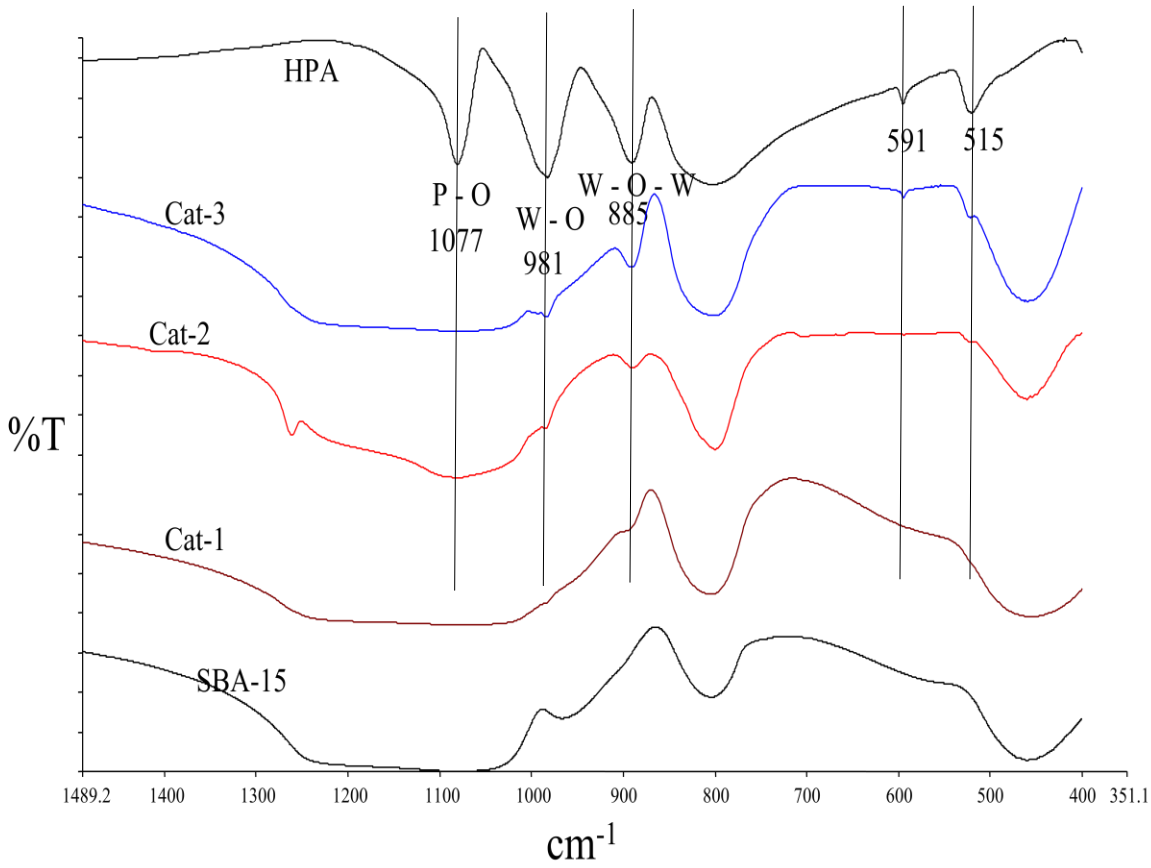

Figure 4.1: FTIR spectra for HPA, SBA-15, Cat-1, Cat-2 and Cat-3.

4.1.3 X-Ray Diffraction analysis

XRD analysis was used to identify the structural morphology and crystalline nature of the support and catalyst. The low angle XRD patterns were shown in Figure 4.2 for the interval between the 2θ = 0.5 - 10°. Three peaks observed at 0.5, 1.1 and 1.6° for SBA-15 were identified as the reflections of three different planes and associated with hexagonal symmetry (Soni et al., 2011). The HPA loaded catalysts also exhibit similar peaks, which confirm that the primary structure of SBA-15 was unchanged during impregnation of HPA and calcination at 300 °C (see Figure 4.2).

The wide angle XRD patterns of the samples at 2θ = 10 - 80° were shown in Figure 4.3. The XRD patterns of HPA shows that it was in crystalline form. When HPA was impregnated on SBA-15, additional peaks were observed for Cat-1, Cat-2 and Cat-3 (see Figure 4.3). This confirms that the HPA was properly deposited on SBA-15 and improved its crystallinity. The peaks at 2θ values of 25.8 and 30.2° were confirmed as cesium tungsten oxide with International Centre for Diffraction Data (ICDD) library. With the increase in HPA loading, the intensity of the peak heights decreased (see 2θ values of 24, 25.8, 30.2, 35 and 38.5° from Cat-1 to Cat-3 in Figure 4.3). The HPA has tungsten (W) as active component and its presence enhances the catalytic activity of the supported catalyst due to the presence of more active acidic sites.

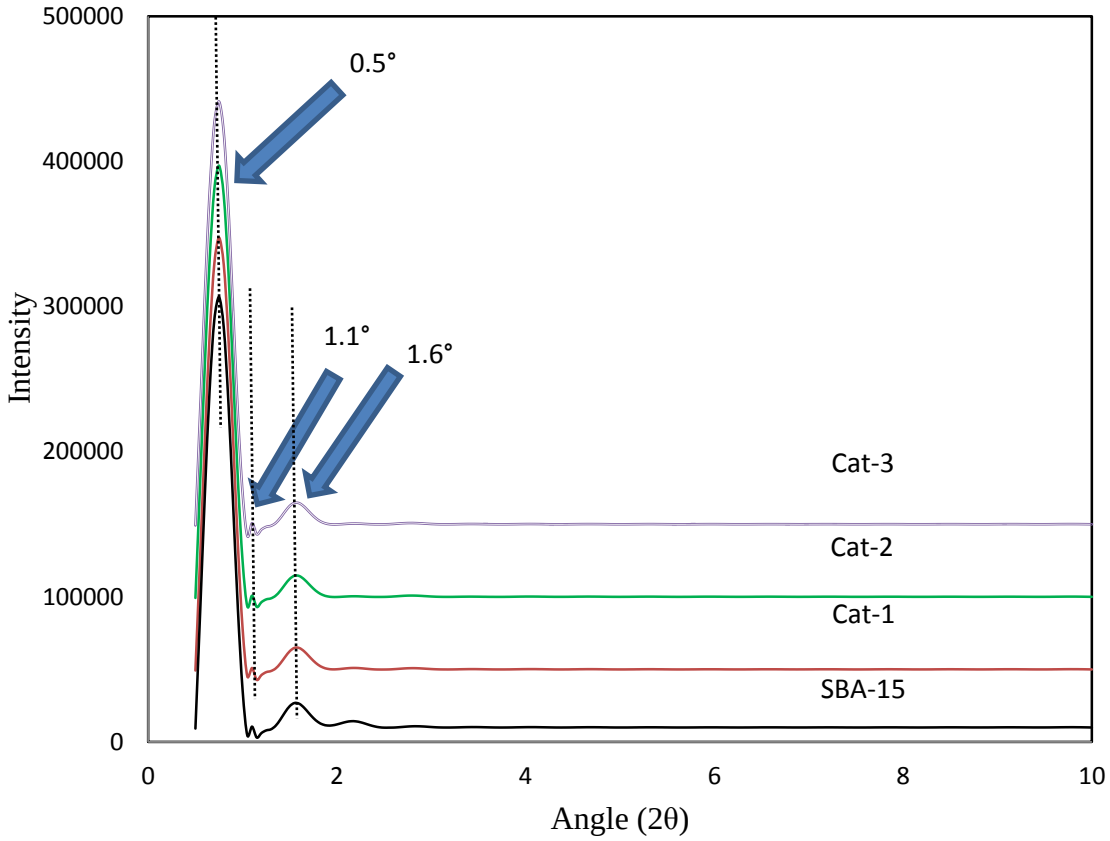

Figure 4.2: Low angle XRD patters for SBA – 15, Cat-1, Cat-2 and Cat-3.

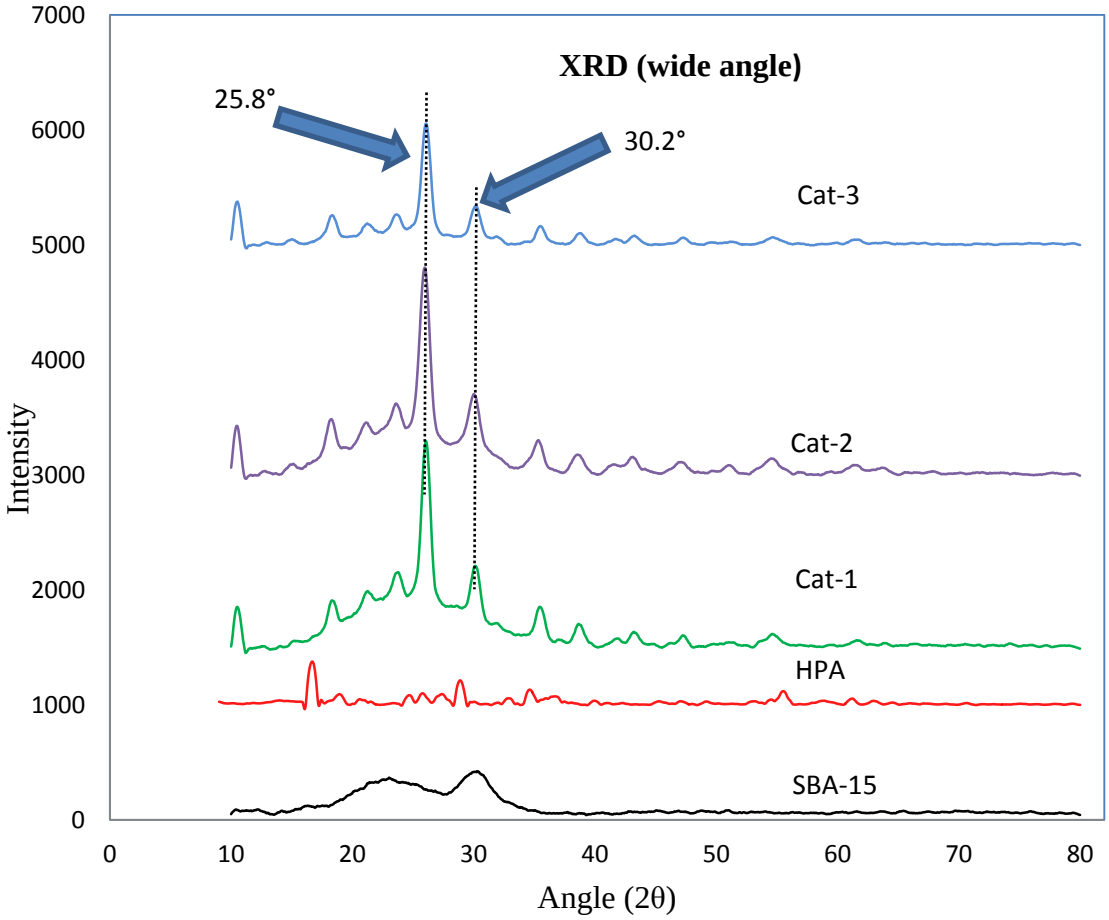

Figure 4.3: Wide angle XRD patterns for HPA, SBA – 15, Cat-1, Cat-2 and Cat-3.

The average crystallite sizes of the different catalyst were calculated by Scherrer's equation (Hosseini et al., 2011) and compared with BET surface area results (see Table 4.2).

$$D_c = \frac{K\lambda}{\beta \cos\theta} - - - -(4.a)$$

D_c - Average cystallite size (nm)

λ - Wavelength of the radiation

β - Integral width of Bragg reflection at 2θ

K - Scherrer constant (0.93)

Table 4.2: Average particle diameters of different catalysts

Sample	**XRD (nm)**	**BET (nm)**
Cat – 1	4.79	4.98
Cat-2	4.65	4.92
Cat-3	4.19	4.85

4.1.4 Thermogravimetric analysis

The weight loss during thermogravimetric analysis was calculated from the ratio of change in weight to the initial weight of the sample. Due to moisture loss, a sudden drop in weight was observed for all samples till 120 °C (see Figure 4.4). Comparatively, lower weight losses were observed in the range of 120 to 500 °C, i.e. 1.09, 1.36 & 1.45 wt % for Cat-1, Cat-2 and Cat-3 samples respectively. It indicates that the catalysts were quiet stable up to 500 °C. Glycerol etherification reactions were performed in the range of 100 to 130 °C. At these reaction temperatures, catalysts were stable as they are calcined at 300 °C prior to the reactions.

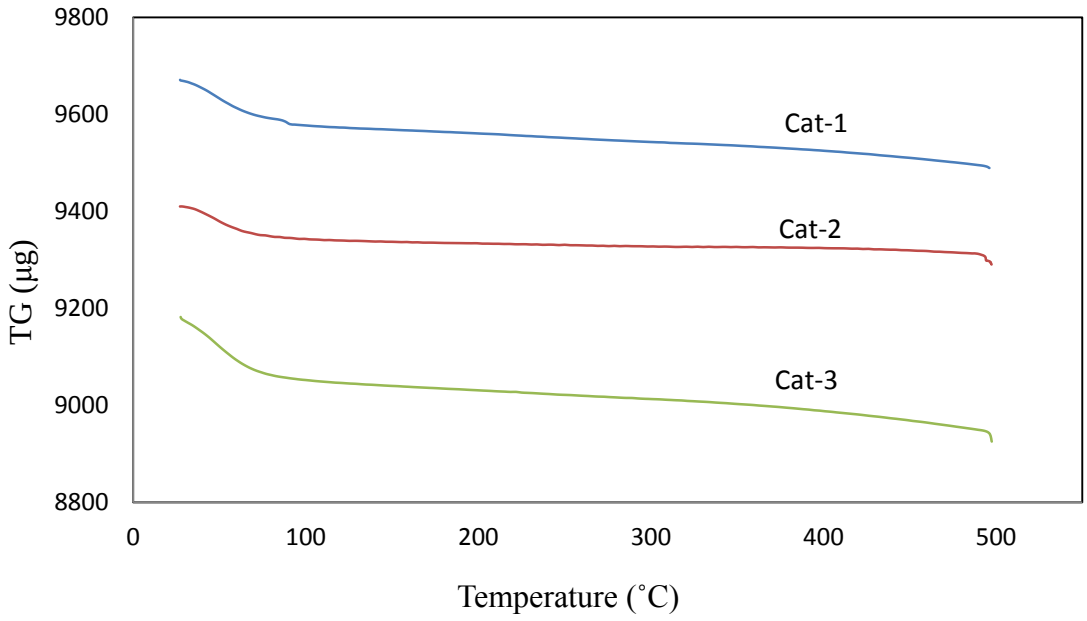

Figure 4.4: Thermogravimetric analyses for Cat-1, Cat-2 and Cat-3.

4.1.5 Scanning Electron Microscopy

The change in SBA-15 structure upon impregnation of HPA was identified using XRD, the significant change in crystal morphology is found in Scanning Electron Microscopy (SEM). The images were captured at 5 µm and 1 µm magnifications for SBA-15, Cat-1, Cat-2 and Cat-3 samples, these were shown in Figuress 4.5, 4.6, 4.7 and 4.8 respectively.

SBA-15 is in amorphous form, which has the pore volume of 1.14 cc/g, the 1 µm magnified SEM image clearly indicate the particle size and void space of the particles (see Figure 4.5). During impregnation of HPA ($Cs_xH_{3-x}PW_{12}O_{40}$, x = 1.5, 2.2 and 2.9), the pores were gradually filled. Hence, at 1 and 5 µm magnification, there was not much change observed for Cat-1, Cat-2 and Cat-3 particles.

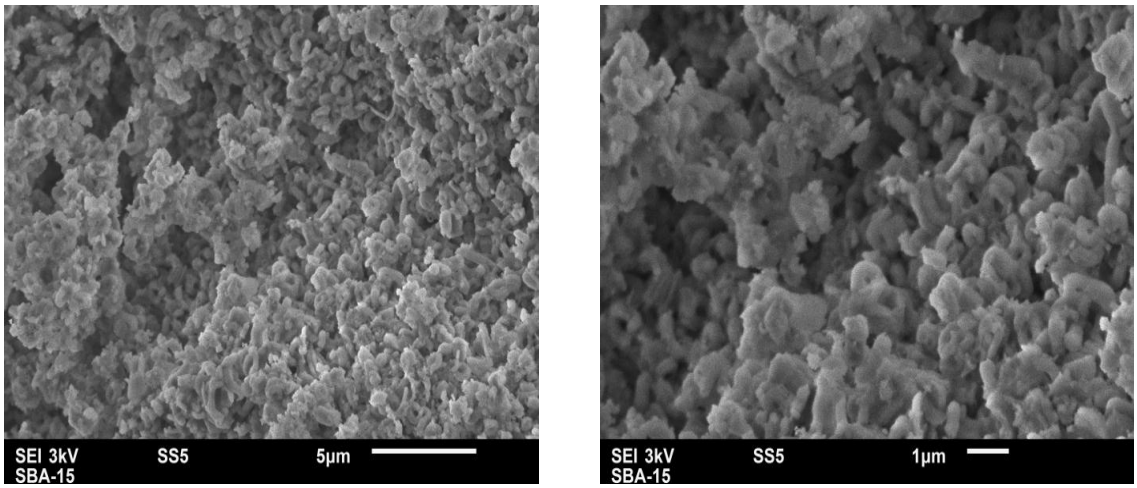

Figure 4.5: SEM image of pure SBA-15

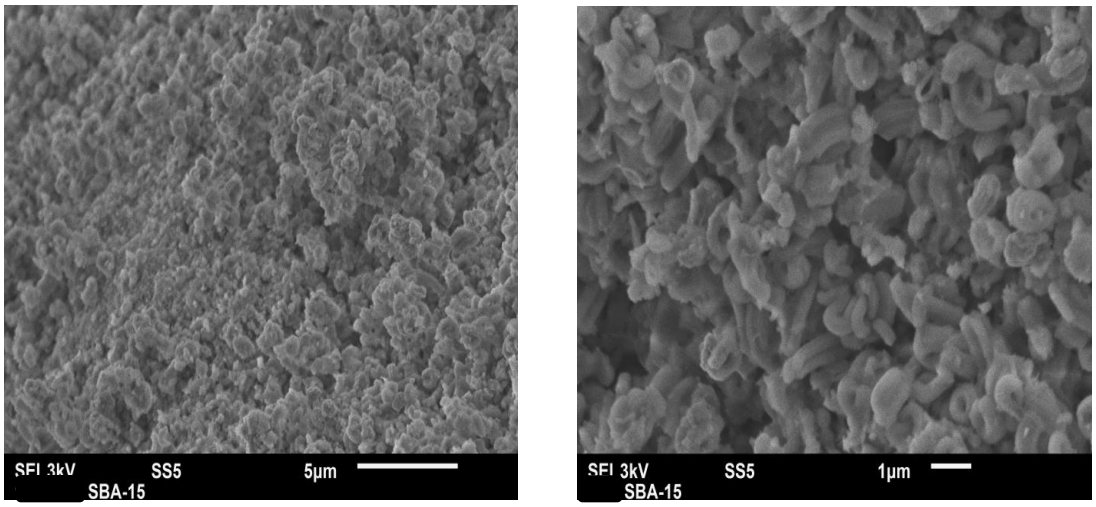

Figure 4.6: SEM image of Cat-1 ($Cs_{1.5}H_{1.5}PW_{12}O_{40}$ on SBA-15)

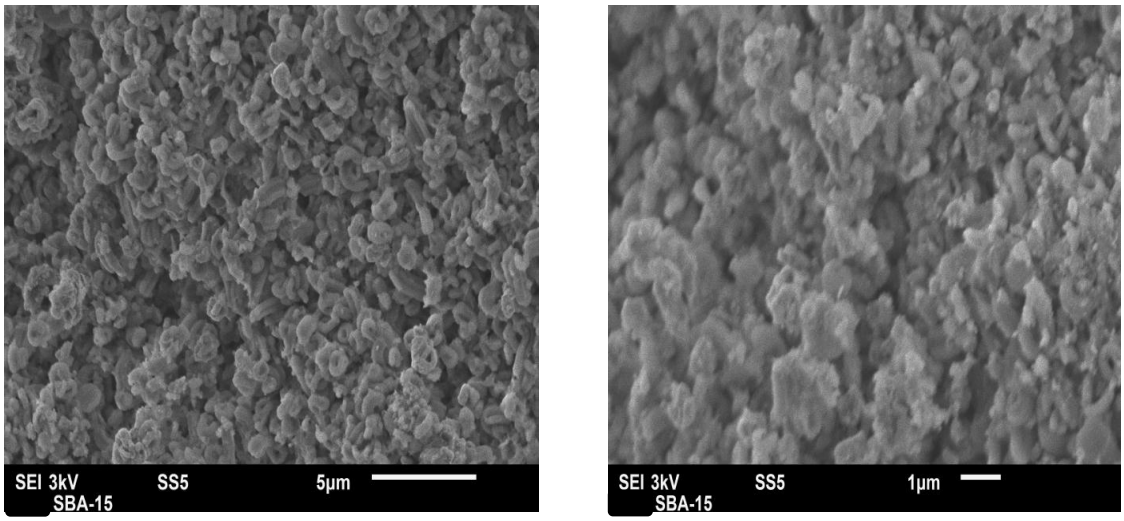

Figure: 4.7 SEM image of Cat-2 ($Cs_{2.2}H_{0.8}PW_{12}O_{40}$ on SBA-15)

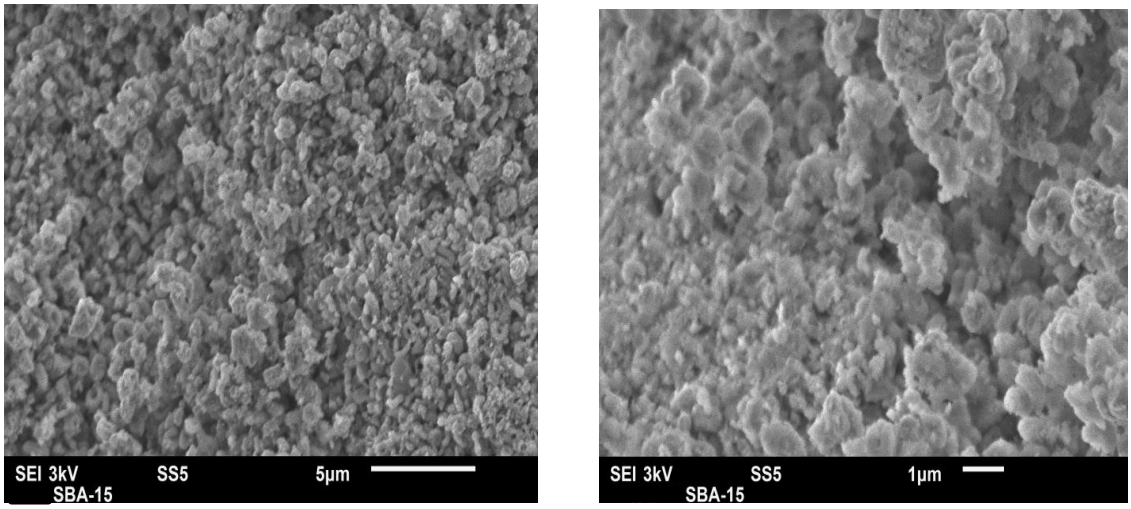

Figure 4.8: SEM image of Cat-3 ($Cs_{2.9}H_{0.1}PW_{12}O_{40}$ on SBA-15)

4.1.6 Elemental analysis

The elemental compositions of HPA supported samples were identified using inductively coupled plasma-mass spectroscopy (ICP-MS). The targeted and measured compositions of Cs and W metal are summarized in Table 4.3. The catalyst samples were found to be stable during calcination at 300 °C for 3 hours.

Table 4.3: Elemental compositions of heteropolyacid supported catalysts

Sample	**Composition (wt %)**			
	Targeted		**Measured**	
	Cs	**W**	**Cs**	**W**
SBA-15	-	-	-	-
Cat-1	1.50	11.60	1.42	10.30
Cat-2	2.20	19.20	2.06	14.92
Cat-3	2.90	27.00	2.59	23.90

4.1.7 Ammonia – Temperature Programmed Desorption

The acidic strength of HPA ($Cs_xH_{3-x}PW_{12}O_{40}$, x = 1.5, 2.2 and 2.9) supported on SBA-15 samples were measured using ammonia-temperature programmed desorption (NH_3-TPD). The analysis was carried out in the range of 50 to 350 °C because the catalyst samples were calcined at 300 °C prior to the reaction. The ammonia desorption peaks were clearly observed and shown in Figures 4.9, 4.10 and 4.11 for Cat-1, Cat-2 and Cat-3 respectively. The adsorbed ammonia started to desorb at 50 °C, with tremendous increase in rate achieving maximum at 110 °C and decreased to minimum at 350 °C. Two peaks identified at 110 and 285 °C are due to the presence of acidic sites. The maximum desorption was identified from the graphs at 110 °C for all catalysts. The variation in HPA loading on SBA-15 doesn't have significant shift in desorption peak. According to Atia et al. (2008), these peaks were confirmed as Bronsted acidic sites. The amount of acidic site concentration was calculated and shown in Table 4.3. With increase in catalyst loading from x = 1.5 to 2.9 % (Cat-1 to Cat-3), the acidic site concentration increased from 0.23 to 0.38 mmol/g (see Table 4.4).

Table 4.4: Ammonia temperature programmed desorption results

Sample	**Acidity (mmol/g)**
Cat-1	0.23
Cat-2	0.33
Cat-3	0.38

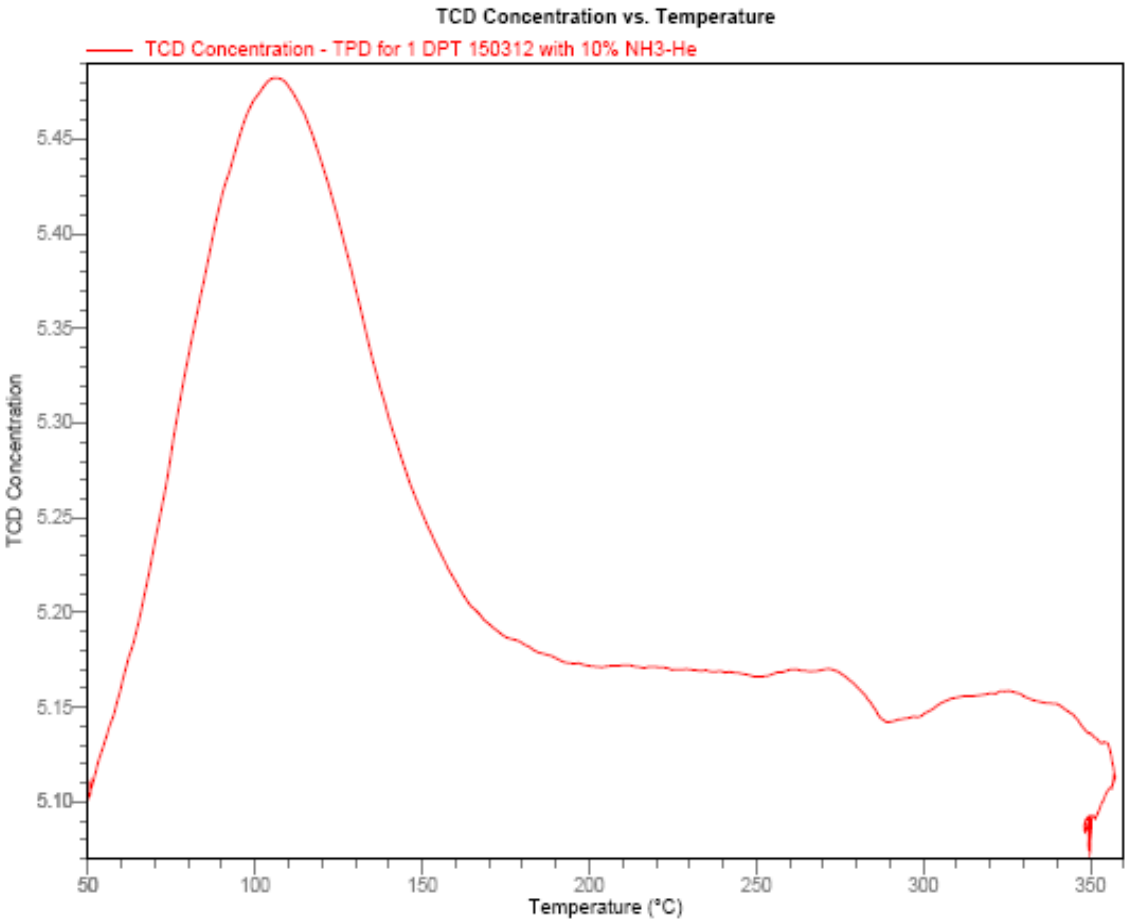

Figure 4.9: Ammonia-temperature programmed desorption (NH_3-TPD) for Cat-1

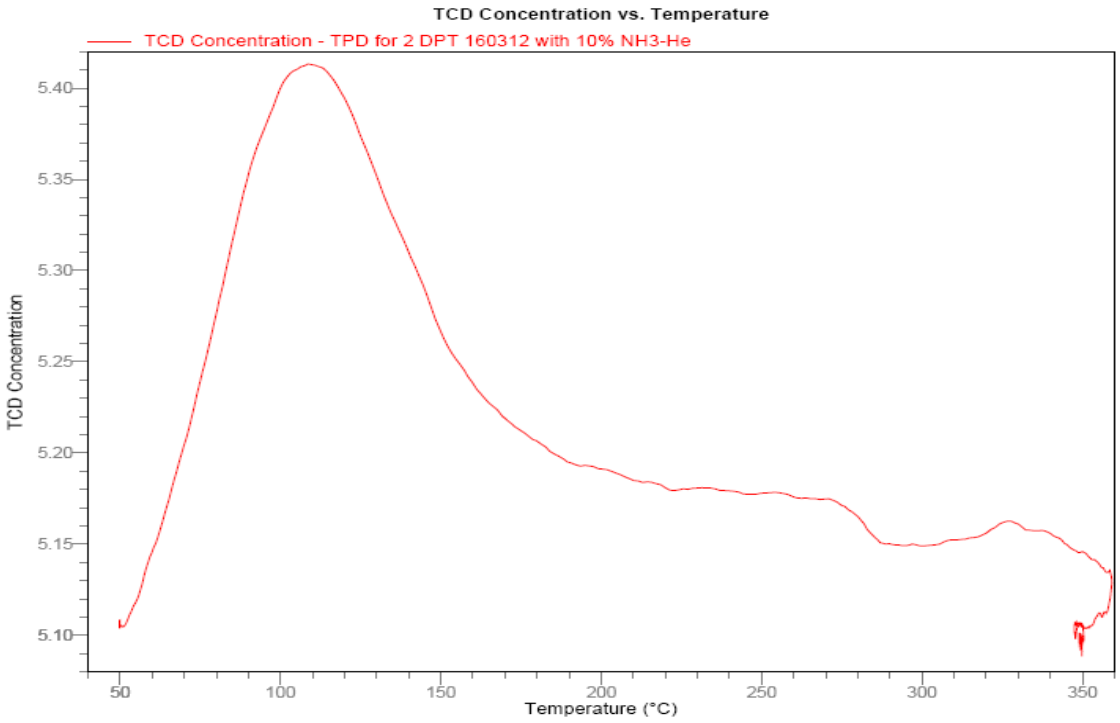

Figure 4.10: Ammonia-temperature programmed desorption (NH_3-TPD) for Cat-2

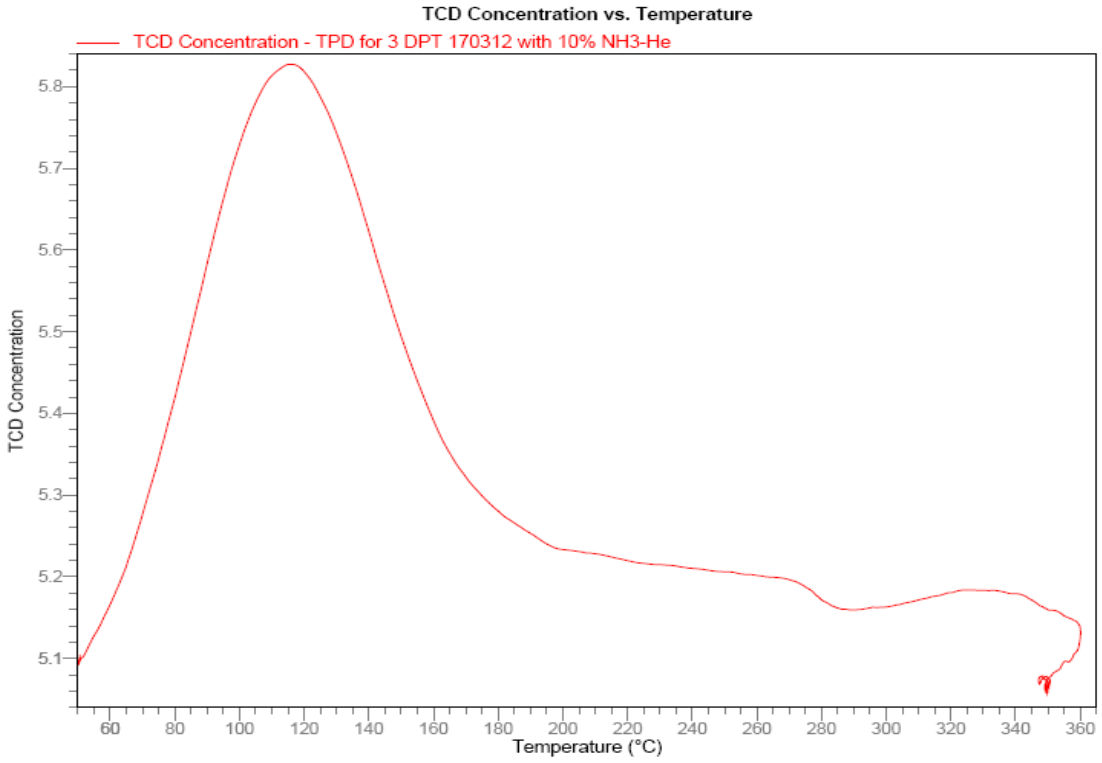

Figure 4.11: Ammonia-temperature programmed desorption (NH_3-TPD) for Cat-3

4.1.8 Measurement of particle size distribution

Particle size of a sample was measured with Mastersizer instrument using optical techniques. The Mastersizer installed with 300 RF lens, which can measure the particle size range of 0.05 – 800 μ m. It has 3 main components, optical unit, sample feeder and a P. C installed with Malvern software. Initially, the sample feeder was cleaned and the obscuration reading of 0 % was confirmed, it indicates that the system was sufficiently purged of particles before measuring the particle size of a sample. The sample was added to the wet feeder and it was confirmed that the obscuration on the screen is within 20%. The ideal obscuration was 10 – 30 %. The sample feeder was connected to the cell at optical unit. In optical unit, laser radiation was emitted, transmitted through beam expander and cell, which was collected by the receiver. The receiver detects the scattering pattern due to presence of particles in the path of laser beam. The Malvern software calculates the particle size distribution based on the scattering and plot against volume %. (see Figure 4.12).

The Thiele modulus (Φ) is directly proportional to the catalyst particle radius (R) (Fogler, 2004), so the catalyst particle size can influence the internal diffusion. In the presence of granular particles (diameter < 100 μ m) the internal diffusion can be negligible (Mao et al., 2008). In the current study, majority of the particles were found in the range of less than 100 μ m. Very less amount of sample was observed for the particle size range of 100 – 800 μ m. The analysis was repeated twice to find the reproducibility, and found that the 94% of the sample had particle size distribution of less than 100 μ m and the remaining 6 % sample had 100 – 800 μ m (see Figure 4.12 and Table 4.5).

For better conclusion on internal diffusion, the Thiele modulus and effectiveness factors were calculated (see Appendix A).

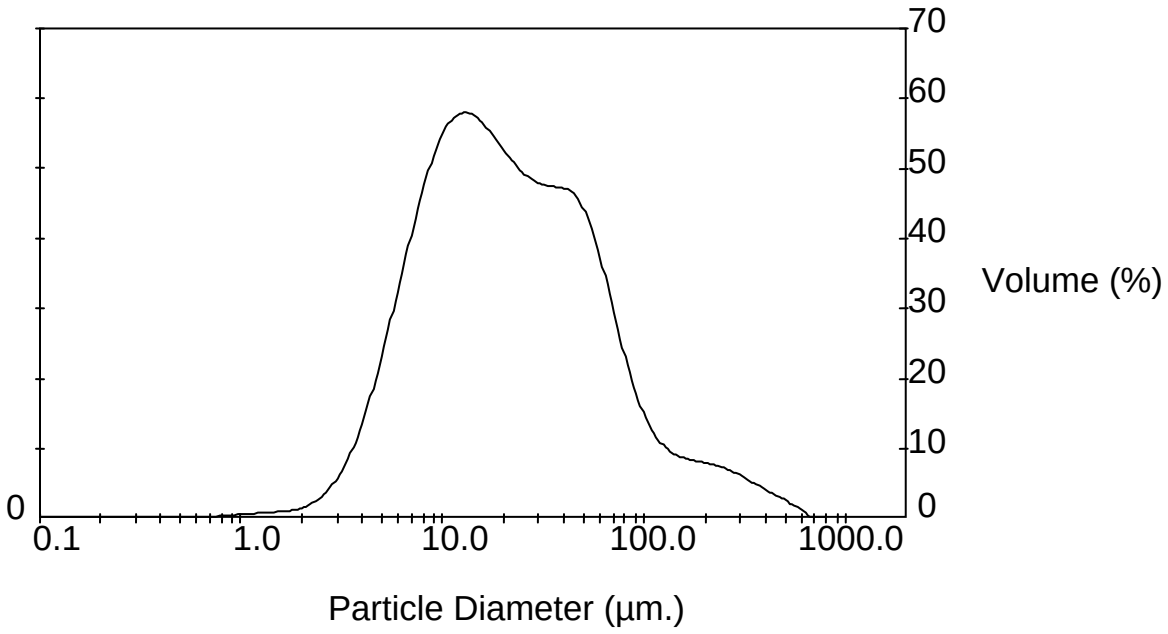

Figure 4.12: Particle size distribution plot (Cat-2)

Table 4.5: Particle size distribution

Particle size (µm)	**Volume (%)**
0.05 – 1	0.14
1.01 – 10	25.60
10.01 – 20	27.56
20.01 – 30	9.77
30.01 – 40	9.46
40.01 – 50	8.93
50.01 – 60	4.71
60.01 – 70	2.95
70.01 – 80	2.20
81.01 – 90	1.60
90.01 – 100	1.21
100.01 – 800	5.87
Total	100.00

4.2 Screening of catalyst loading on support

Prior to the catalyst screening studies, a blank run was performed without any catalyst. There was no significant change in glycerol conversion (~ 3 mol %) was observed. Then another run was performed with heteropolyacid (conditions: 120 °C, 1 MPa, 1:5 molar ratio (glycerol/TBA), 0.5 g of HPA and 800 rpm). HPA is soluble in alcohol and homogeneous reaction mixture was observed. The glycerol conversion was found to be 68 mol % at 4 hours, but at the end of the reaction the dissolved HPA could not be separated. In order to inhibit the solubility of HPA, the proton was exchanged with Cesium and was made insoluble (Park et al., 2010).

The screening studies were performed at 110 and 120 °C with Cat-1, Cat-2 and Cat-3. The reaction conditions were maintained at 1 MPa, 2.5% (w/v) catalyst loading, 1:4 molar ratio (glycerol/TBA) and 800 rpm. The percentage conversion of glycerol was calculated and summarized in Table 4.6. To test for repeatability, reaction was performed twice at 120 °C with Cat-2.

The conversion of glycerol was influenced by HPA loading. Cat-1 shows low conversion of glycerol at both temperatures of 110 and 120 °C due to low catalyst loading (x = 1.5, $Cs_xH_{3-x}PW_{12}O_{40}$). As the loading increased from x = 2.2 (Cat-2) to 2.9 (Cat-3), the catalytic activity increased. The conversion of glycerol is directly proportional to the available active sites (Yadav et al., 2011). At 120 °C, the glycerol conversion at 67 minutes for Cat-3 was 43 %, which was much higher than that for Cat-2 (36%). But, for Cat-2 and Cat-3, the difference between glycerol conversions at 247 minutes was 4 %. For Cat-2, higher conversion of glycerol 58.4 % was found at 247 minutes though the

conversion was only 10.5 % at 7 minutes. Therefore, the required catalyst was selected for maximum conversion of glycerol with slower reaction rate. So Cat-2 was chosen for further investigation for optimization study.

Table 4.6: Conversion of glycerol (mol %) as a function of time at 110 and 120 °C with different catalysts (Conditions: 1 MPa, 2.5% (w/v) catalyst loading, 1:4 molar ratio (glycerol/TBA) and 800 rpm)

Temperature (˚C)	**Catalyst**	**Glycerol conversion with time (minutes)**				
		7	**67**	**127**	**187**	**247**
110	Cat-1	4.3	14.0	20.1	27.0	32.0
110	Cat-2	8.7	30.9	41.5	49.4	53.0
110	Cat-3	11.4	38.6	47.9	56.3	59.3
120	Cat-1	6.5	18.2	26.7	33.1	38.4
120	Cat-2	10.5	36.3	45.5	53.7	58.4
120	Cat-3	13.3	43.4	52.9	59.6	62.2

4.3 Estimation of process parameters

The etherification of glycerol with TBA reaction was studied for maximum conversion of glycerol. The effect of process parameters such as reaction temperature, catalyst loading, molar ratio (glycerol/TBA) on glycerol etherification was studied and the conditions were optimized for the maximum conversion of glycerol. Also, the effect of transport limitations on the reaction as described below. In order to make sure that the reactants are in liquid phase, the pressure inside of the reactor was maintained at 1 MPa (with N_2) for different temperature (100 – 140 °C) conditions (Rattanaphra et al., 2012).

4.3.1 Effect of transport limitations

In heterogeneous catalysis, the mass and heat transfer resistances play an important role and greatly influence the conversion. The transport limitations were examined prior to the experiments in order to determine its effects on conversion of glycerol.

4.3.1.1 Mass transfer

The mass transfer resistance was due to transport of reactants from bulk fluid to the external surface of the catalyst (external diffusion) and diffusion of the reactant from the external surface to the internal surface (internal diffusion) through catalyst pore mouth (Fogler. 2004). The effect of external diffusion was studied with the change in speed of agitation. Etherification of glycerol reactions are performed for the stirrer speed at 400, 800, 1000 and 1200 rpm and other reaction conditions were maintained at 120 °C, 1 MPa, 1:5 molar ratio (glycerol/TBA) and 2.5 wt% of catalyst loading. As the stirrer speed increased from 400 to 800 rpm, the percentage conversion of glycerol increased from 58 to 71% (see Figure 4.13). It indicates that the external diffusional resistance was overcome by increasing the speed of stirring. The change in glycerol conversion is only

0.5% indicating that the external diffusional resistance is negligible when stirring speed increased from 800 to 1200 rpm. Therefore, 800 rpm was taken as optimum stirrer speed and the optimization studies were performed on this basis.

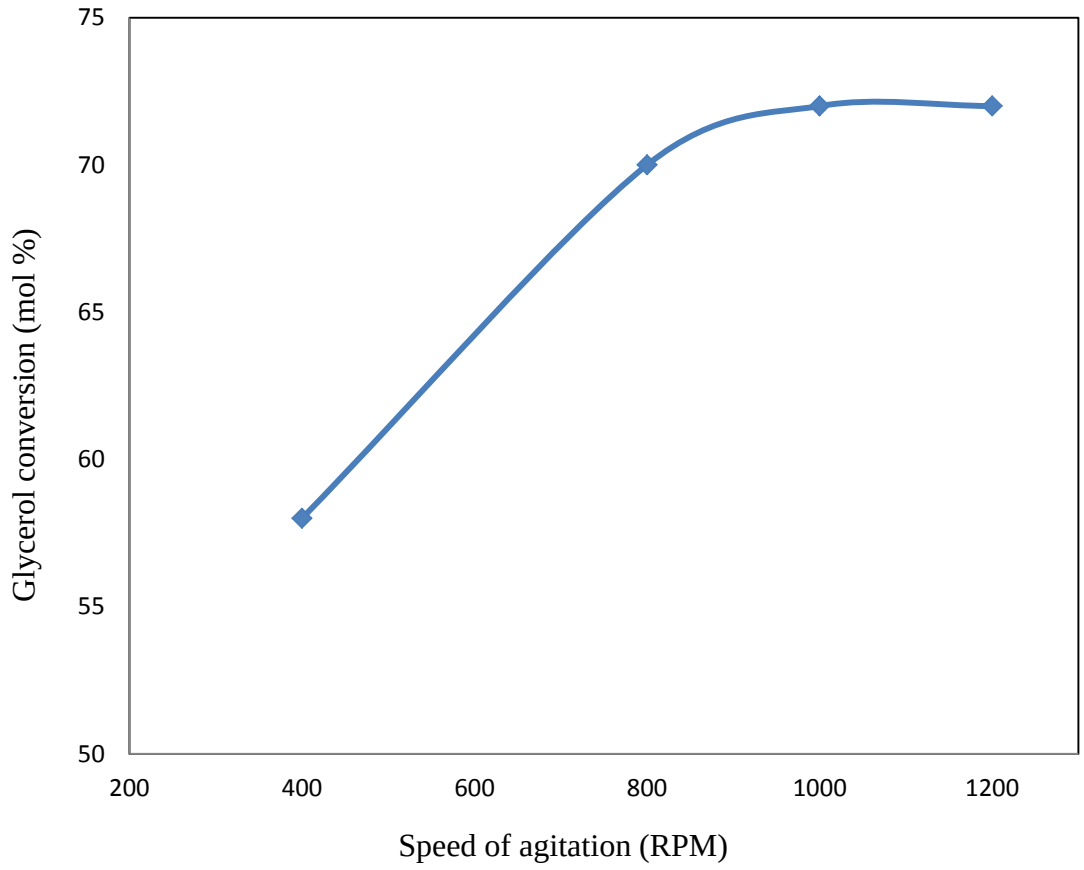

Figure 4.13: Effect of agitation on etherification of glycerol

The effect of internal diffusion on conversion of glycerol was studied by the Thiele modulus (Φ) and effectiveness factor (η) calculations (see appendix: A). The effectiveness factor is defined as the ratio of actual overall rate of reaction to the rate of reaction that would result if entire interior surface was exposed to the external pellet surface conditions (Fogler. 2004).

$\Phi > 3$ and $\eta < 0.3 \rightarrow$ Internal diffusion limits the reaction

$\Phi < 3$ and $\eta > 0.7 \rightarrow$ Surface reaction limits the reaction

The value of Thiele modulus (Φ) was found as 0.686 and the effectiveness factor (η) was 0.972. Therefore, the mass transfer resistance due to internal diffusion was neglected.

4.3.1.2 Heat Transfer

In chemical reactions heat transfer plays an important role by providing the heat required for the reaction. It also generates temperature gradient between catalyst and reactants. The heat transfer can be described in three phases, intra-particle, inter-particle and inter-phase transfer. In heterogeneous catalysis the change in conversion due to intra particle heat transfer was less than 5% (Veldsink et al., 1995). So here the conversion of glycerol due to heat transfer inside catalyst particle was neglected and rest of the reactions are carried out on this assumption. The heat transfer between particles helps to increase the kinetic energy of the reactant species. At higher temperature, more amount of energy is given to reactant molecules; it increases the number of effective collisions in the reaction mixture (Hermida et al., 2011). The inter particle heat transfer was studied for the temperature ranges of 100 to 130 °C (see effect of temperature). Glycerol is soluble in tert-butanol, so the reaction takes place in liquid phase and hence the inter phase heat transfer can be neglected.

.

4.3.2 Effects of temperature

The effects of temperature on etherification of glycerol was studied in the range of 100 – 130 °C by keeping the other reaction parameters constant at 1 MPa N_2 pressure, 1:5 molar ratio (glycerol/TBA), 800 rpm and 3% (w/v) catalyst loading. Etherification of glycerol is a reversible reaction which has slower reaction rate at lower temperature (Klepacova et al., 2003). With increase in temperature from 100 to 130 °C, the percentage of conversion was increased from 43 to 80 % (see Figure 4.14). With the increase in temperature from 100 to 130 °C, more amount of heat was transferred to glycerol and TBA, causing increased inter molecular collisions. Presence of active sites on the catalyst; the effective collisions at higher temperature can aid in the formation of MTBGE (Hermida et al., 2011). At 130 °C, the reaction rate was higher with 59% of glycerol conversion as compared to that with 41 % conversion at 120 °C in 1 hr. One reaction was also performed at 140 °C. At this temperature 65% of glycerol conversion was achieved within one hour and 88% conversion in 4 hours.

Etherification of glycerol with TBA can produce two mono, two di and one tri tert-butyl glycerol ethers (see Figure 2.3) (Frusteri et al., 2009). During gas chromatography analysis, the mono and di isomers are identified as single peaks, so only three product peaks were observed. The mono, di and tri tert-butyl glycerol ethers are named as MTBGE, DTBGE and TTBGE respectively. The effects of temperature on yield of ether were given in Figure 4.15. The yields of MTBGE, DTBGE and TTBGE at 120 °C and 130 °C are 57, 15, 4 and 55, 18, 6 % respectively. It indicates that the yield of MTBGE is maximum at 120 °C, and at 130 °C the yields of DTBGE and TTBGE are increased at the cost of MTBGE yield. It indicates that the MTBGE was the primary product and further

rise in temperature helps MTBGE to react with TBA. So the higher temperatures of 130 and 140 °C were preferred for the production of DTBGE and TTBGE. In current study, the process was optimized for MTBGE, and its yield was maximum 57% at 120 °C; therefore catalyst loading studies were performed at this temperature.

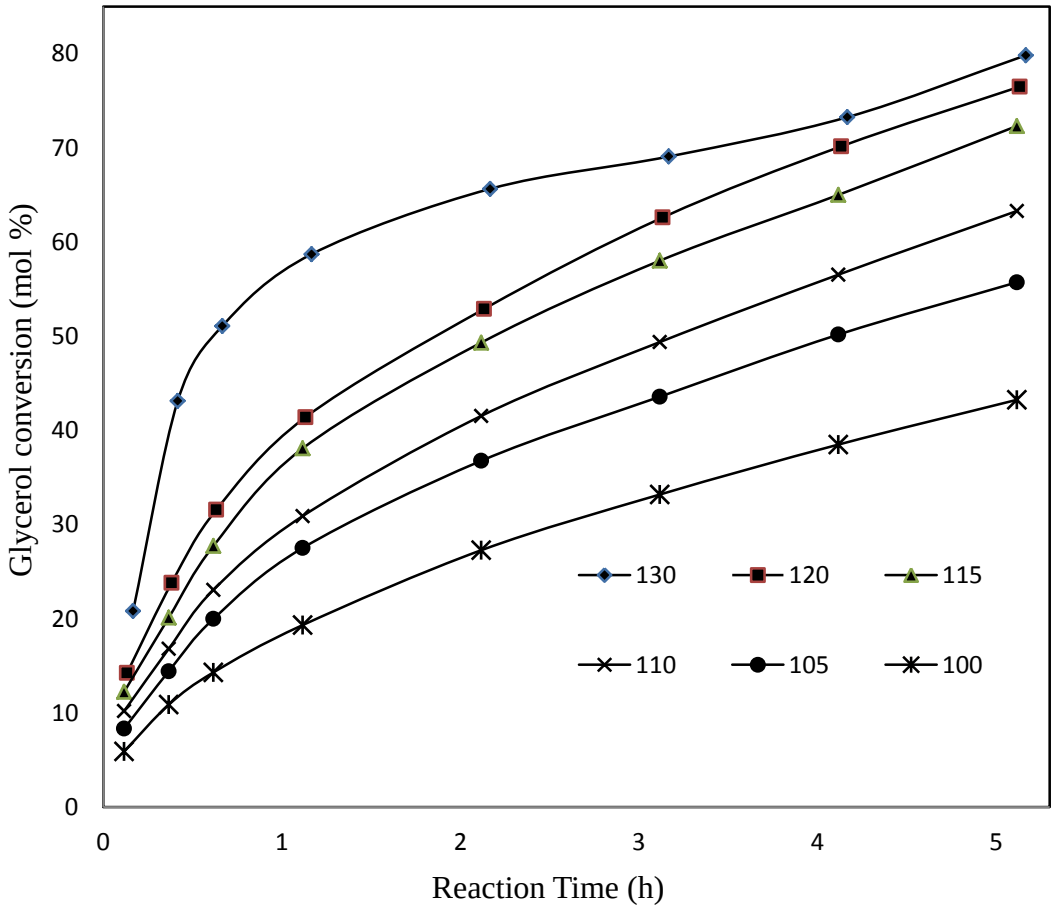

Figure 4.14: Effect of temperature on glycerol conversion at 1 MPa, 1:5 molar ratio (glycerol/TBA), 3% (w/v) catalyst loading and 800 rpm.

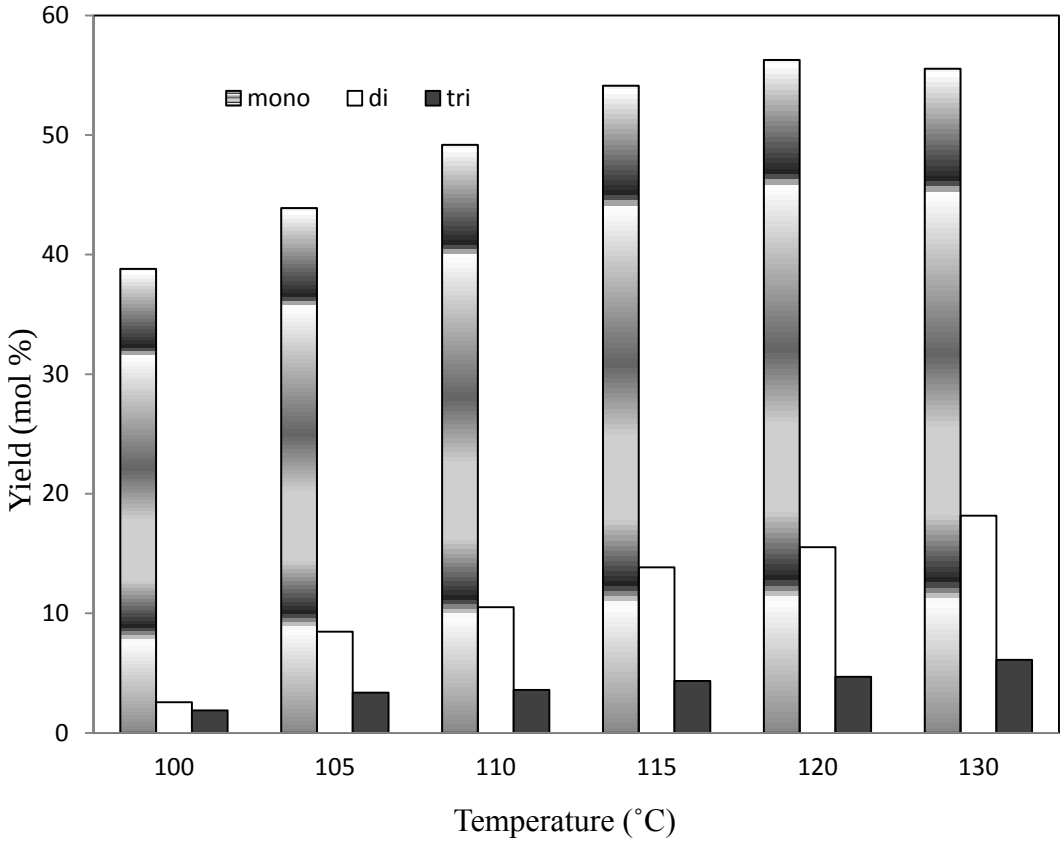

Figure 4.15: Comparison of yields at different temperatures (reaction conditions: 1 MPa, 1:5 molar ratio (glycerol/TBA), 3% (w/v) catalyst loading, 800 rpm and 5 hours).

4.3.3 Effects of catalyst loading

The effect of catalyst loading on glycerol conversion was studied by varying it from 0.5 to 4 % (w/v). The reaction conditions were maintained at 120 °C, 1 MPa, 1:5 molar ratio (glycerol/TBA) and 800 rpm. The number of active sites in the reaction mixture was directly proportional to the amount of catalyst loading (Yadav et al., 2011). The catalyst has the active site concentration of 0.33 mmol/g. The increase of catalyst loading 0.5 to 4% increased the glycerol conversion 42 to 77% (see Figure 4.16). The percentage conversion of glycerol at one hour for 4 wt% loading was much higher than for 3 wt% loading. However, no significant difference was observed in glycerol conversion at 5 hr for 3 and 4 % of loadings. Similar trend was reported by Hermida et al., 2011 for esterification of glycerol.

The effects of catalyst loading on yield of ether were shown in Figure 4.17. The yields of MTBGE, DTBGE and TTBGE at 3 and 4 % (w/v) of loadings were 60, 12, 5 and 56, 16, 6 % respectively. It was observed that the yield of MTBGE was decreased with the increase of loading from 3 to 4 % (w/v). So it is concluded that the 3 % (w/v) of catalyst loading was preferable for higher conversion of glycerol and MTBGE yield. Therefore, it was taken as optimum catalyst loading and further reactions were carried out at these conditions.

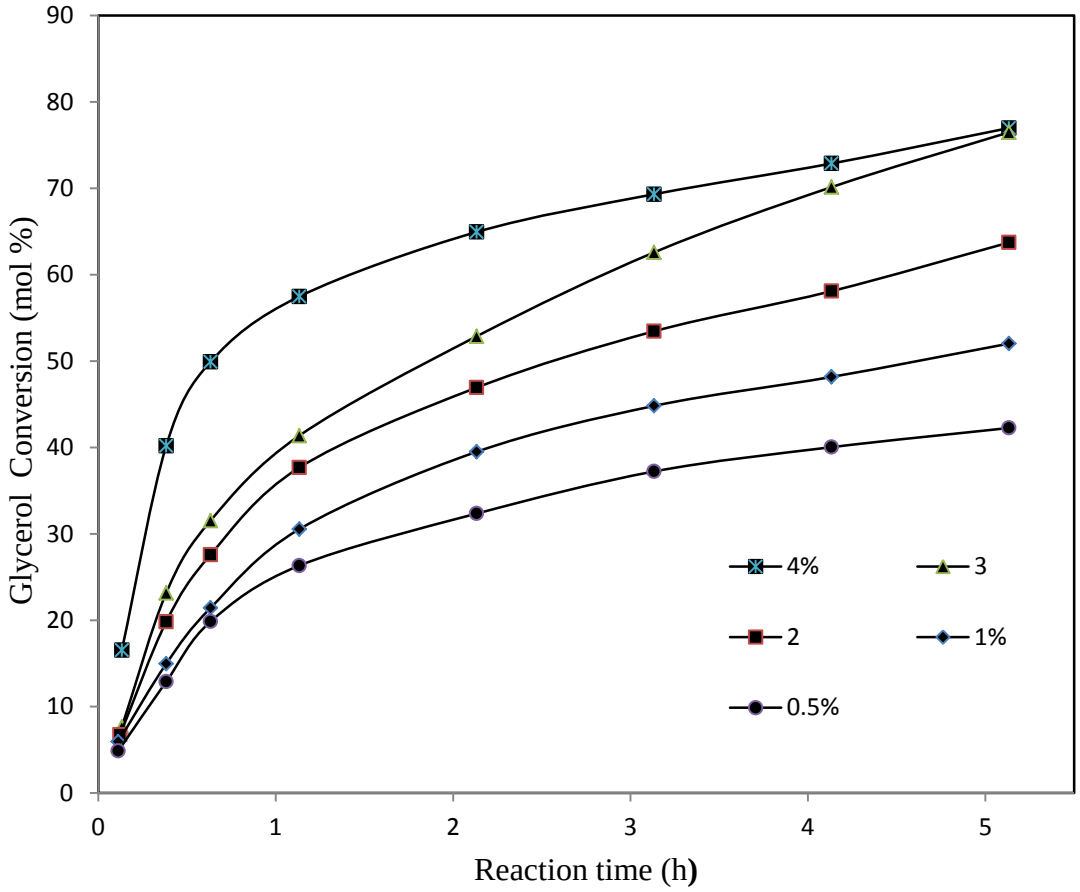

Figure 4.16: Effect of catalyst loading on glycerol conversion at 120 ˚C, 1 MPa, 1:5 molar ratio (glycerol/TBA) and 800 rpm.

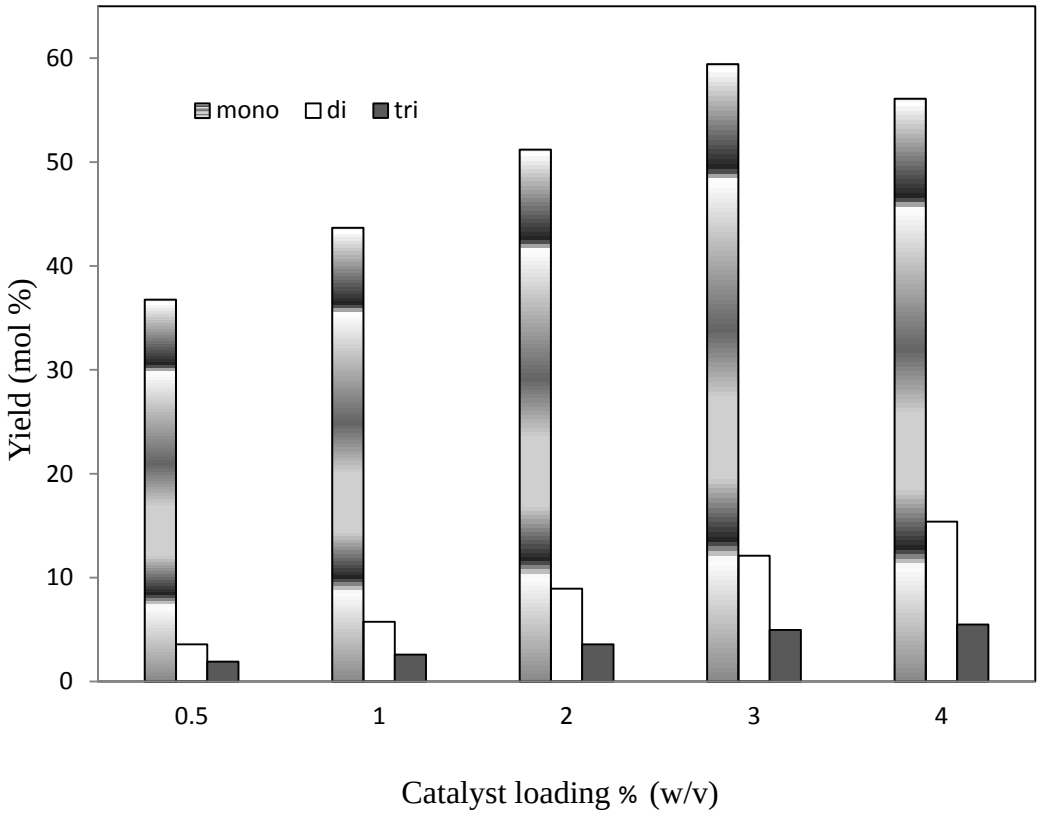

Figure 4.17: Comparison of yields at different catalyst loading for the conditions of 120 ˚C, 1 MPa, 1:5 molar ratio (glycerol/TBA), 800 rpm and 5 hours.

4.3.4 Effects of molar ratio

The effect of glycerol to TBA molar ratio was studied in the range of 1:3 to 1:8. The reaction conditions were maintained at 120 °C, 1 MPa, 3% (w/v) catalyst loading and 800 rpm. The percentage conversion of glycerol at 5 h increased with the change in molar ratio from 1:3 to 1:5, no significant difference was observed for 1:5 to 1:8 molar ratio (see Figure 4.18).

At 1:3 molar ratio, the reaction mixture is viscous because of the presence of less solvent (tert-butanol). The increment of glycerol to solvent molar ratio from 1:3 to 1:5 increased the glycerol conversion from 55 to 76 % and MTBGE yield from 42 to 53% (see Figure 4.18 and 4.19). With the increase in molar ratio from 1:3 to 1:5, the viscosity of the reaction mixture decreased, the mass transfer becomes easier and maximum (Karinen and Krause, 2006). But, further increment of molar ratio to 1:8 increased the glycerol conversion up to 80 % and however decreased the MTBGE yield to 49% (see Figure 4.19). According to Hermida et al., 2011, glycerol etherification reaction takes place at the pores of the catalyst, so the product MTBGE remains in pores. With the presence of excess TBA, it was further etherified to DTBGE and TTBGE. Finally, the maximum yield of MTBGE was obtained at 1:5 molar ratio, beyond which its effect was minimum. Similar behaviour was explained by Zhao et al., (2010) for etherification of glycerol with isobutylene in the molar ratio ranges of 1:2 to 1:5 (glycerol/isobutylene). The increase in mono ether yield was reported from 1:2 to 1:4 molar ratio and decreased slightly from 1:4 to 1:5 molar ratio.

The change in volume during reaction is calculated on the basis of mass balance. There is no change in initial and final volume of the reaction mixture is observed (see Appendix: E). Therefore, the volume is constant throughout the reaction.

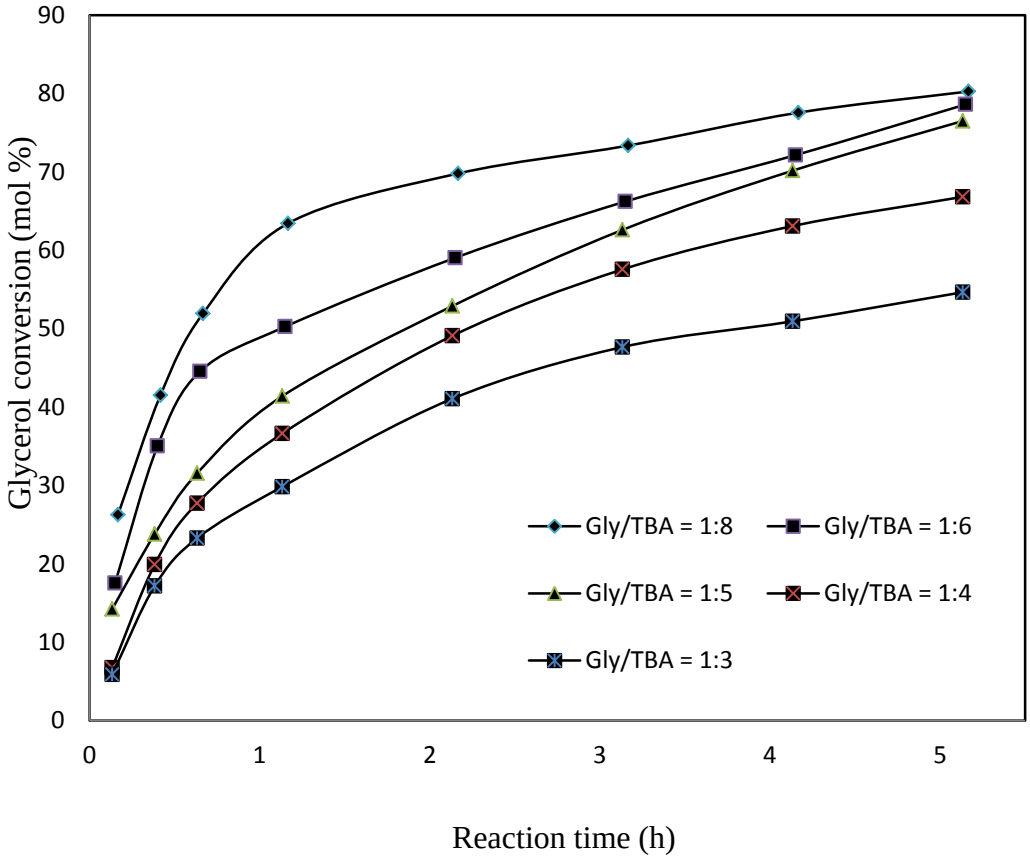

Figure 4.18: Effect molar ratio on glycerol conversion at 120 ˚C, 1 MPa, 3% (w/v) catalyst loading and 800 rpm.

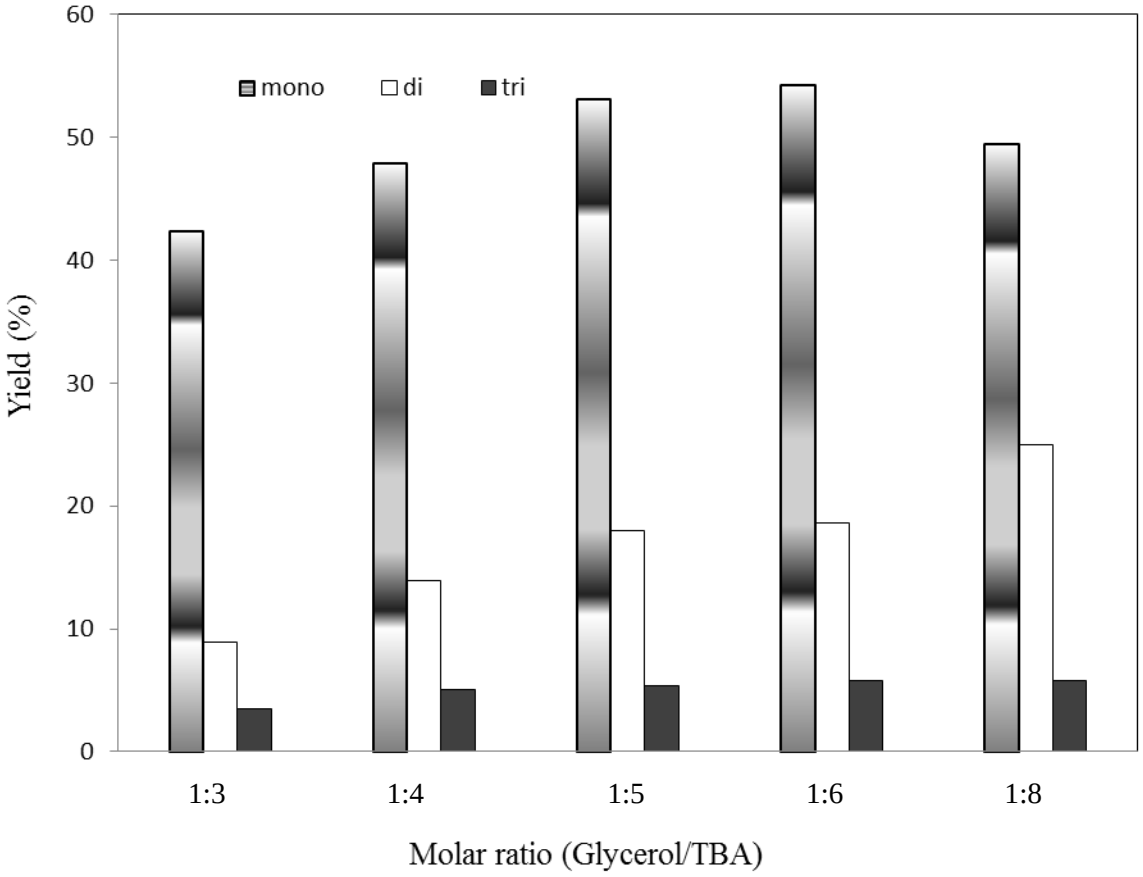

Figure 4.19: Comparison of yields at different molar ratio (glycerol/TBA) for the reaction conditions of 120 ˚C, 1 MPa, 3% (w/v) catalyst loading, 800 rpm and 5 hours.

4.3.5 Catalyst re-usability

The catalyst was separated from the reaction mixture through filtration, dried at 120 °C for 4 hours and calcined at 300 °C for 3 hours. The catalyst was weighed after calcination and found 5% of weight loss. It was due to attrition of the catalyst particles during mixing, handling in filtration and reloading, so the make-up amount was added and the catalyst was used for second run. Similar procedure was repeated for third run and it was found that the conversion of glycerol decreased from 76 to 73 % after three uses (see Figure 4.20). During drying and calcination, some adsorbed species deposit in the pore structure which was reflected in the change of glycerol conversion. The catalyst was stable and active up to 3 runs. Long term deactivation study has not been performed on this catalyst.

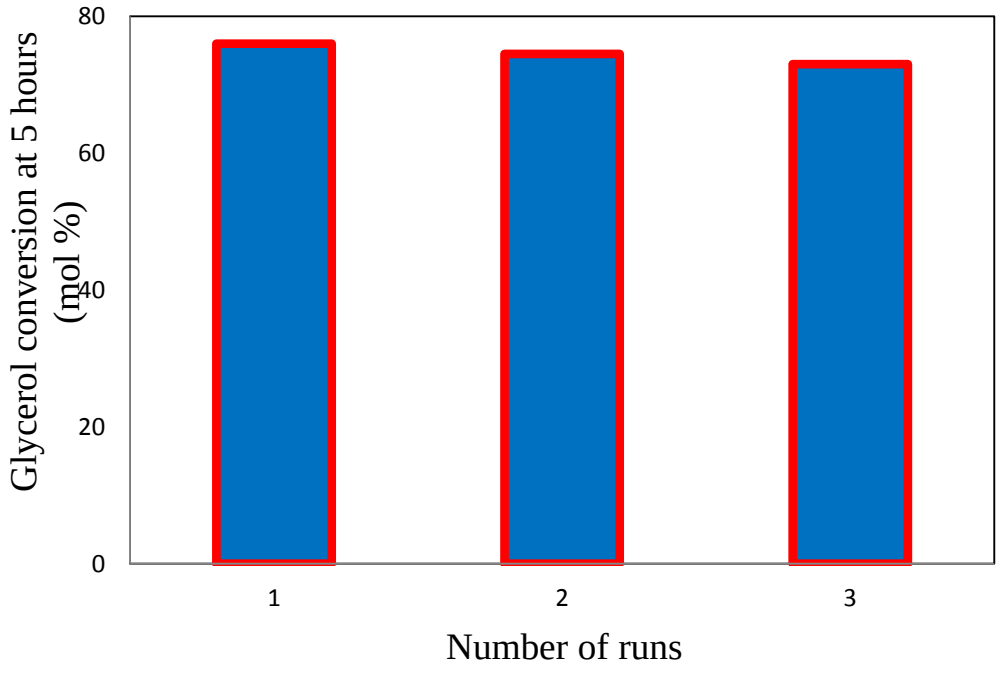

Figure 4.20: Catalyst re-usability study

4.4 Kinetic study

The optimized results were used to develop a kinetic model for etherification of glycerol. In this reaction, glycerol (G) and TBA (T) react to produce MTBGE (M) and water (W) as products.

Assumptions for selection of a kinetic model (Satterfield, 1991)

1. The reactants (G, TBA) and products (MTBGE, W) are appreciably adsorbed on the catalyst surface.
2. The rate of reaction is directly proportional to the product of the concentration of adsorbed glycerol and adsorbed TBA.
3. No dissociation of glycerol and TBA occurs on adsorption.
4. The reverse reaction is negligible.
5. One active site used for the adsorption of one species only.

From the assumptions, adsorption, surface reaction and desorption steps are identified as crucial in developing a kinetic model. The power law model does not include the aspects of adsorption or desorption of reactants and products, and inhibition by reactants/products while calculating the reaction rate. Therefore, the power law model was excluded due to above limitations (Ramachandran and Chaudhari, 1983). According to Langmuir-Hinshelwood kinetics, the adsorption of glycerol and TBA, surface reaction, desorption of mono ether and water are considered in the derivation of the mathematical model (Fogler, 2004).

4.4.1 Derivation of rate equation using Langmuir-Hinshelwood kinetics

Step: 1a Adsorption of glycerol is written as

$$G + S \underset{k_{-1}}{\overset{k_1}{\rightleftharpoons}} G.S \quad ----------(4.1)$$

Step: 1b Adsorption of TBA is written as

$$T + S \underset{k_{-2}}{\overset{k_2}{\rightleftharpoons}} T.S \quad ----------(4.2)$$

Step: 2 Surface reaction of the G.S and T.S leads to form MTBGE (M.S) and water (W.S) on the vacant site.

$$G.S + T.S \underset{k_{-3}}{\overset{k_3}{\rightleftharpoons}} M.S + W.S \quad ----------(4.3)$$

Step: 3 Desorption of M.S and W.S is written as

$$M.S \underset{k_{-4}}{\overset{k_4}{\rightleftharpoons}} M + S \quad ----------(4.4)$$

$$W.S \underset{k_{-5}}{\overset{k_5}{\rightleftharpoons}} W + S \quad ----------(4.5)$$

For the remaining part of the derivation see Appendix: B

$$\ln \frac{(M - X_G)}{M(1 - X_G)} = (M - 1)\, k\, {w_t}^2\, C_{G0}\, t, \qquad M \neq 1 \quad ----(4.6)$$

This is the desired integrated rate equation for second order reaction with $C_{G0} \neq C_{T0}$ in terms of conversion.

k_t= constant

w_t = catalyst loading

C_{G0} and C_{T0} are the initial concentrations of glycerol and tert-butanol.

Let $M = \frac{C_{T0}}{C_{G0}}$ = the initial molar ratio of reactants

C_G and C_T are the concentrations of glycerol and tert-butanol at any time t.

Amount of glycerol reacted = $C_{G0}\, X_G$

Amount of tert-butanol reacted = $C_{T0}\, X_T$

$\ln \frac{(M - X_G)}{M\,(1 - X_G)}$ vs t is plotted at different temperatures (100 to 120 °C) (see Figure 4.21).

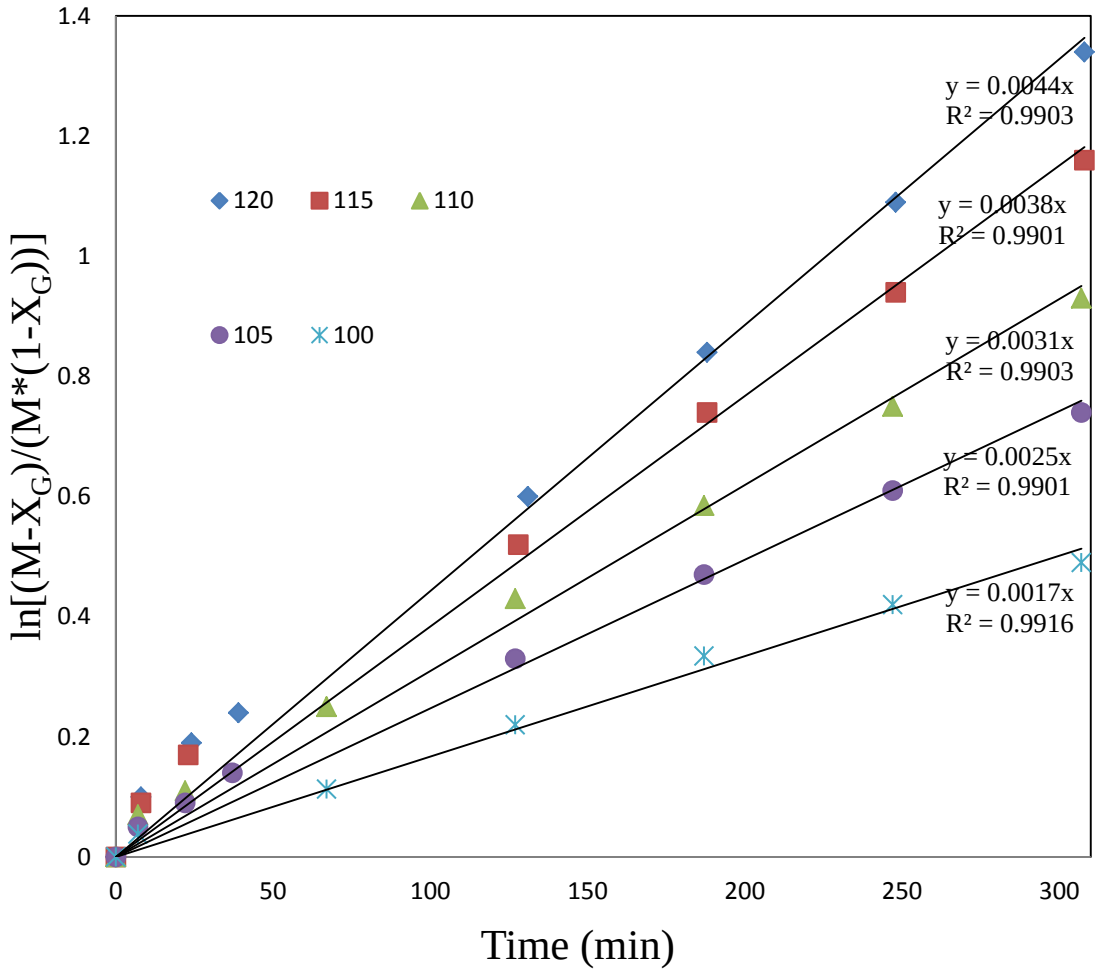

Figure 4.21: Plot of $\ln \frac{(M - X_G)}{M\,(1 - X_G)}$ vs time at different temperatures

The average R^2 value of 0.99 in the range of 100 - 120 °C shows that the data fit linearly. So the glycerol etherification reaction follows the second order kinetics. The rate constants are calculated for second order reaction from 100 to 120 °C and shown in Table 4.7.

Table 4.7: Rate constant at different temperatures

Temperature (T)			**Rate constant (k)**	**ln(k)**	**ln(k/T)**
°C	**K**	**1/T**	**(l/mol) min^{-1}**		
120	393	0.002545	0.0052	-5.26	-11.23
115	388	0.002577	0.0042	-5.47	-11.43
110	383	0.002611	0.0030	-5.81	-11.76
105	378	0.002642	0.0021	-6.17	-12.10
100	373	0.002681	0.0015	-6.51	-12.43

Glycerol etherification is an endothermic reaction, so the rate constant is found to increase with temperature (see Table 4.7).

4.4.2 Arrhenius plot for kinetic model

The energy of activation for etherification of glycerol is determined by Arrhenius plot (see Figure 4.22)

$$k = k_0 \exp(-E/RT) \quad (4.7)$$

$$\ln k = \ln k_0 - E/RT \quad (4.8)$$

$k_0 \rightarrow$ Frequency factor

$E \rightarrow$ Activation Energy

$R \rightarrow$ Gas constant

$T \rightarrow$ Temperature

The data $\ln k$ vs $1/T$ (see Table 4.7) is plotted in Figure 4.22 with the slope of the line equal to $-E/R$ which shows an activation energy of $78\ kJ/mol$. See Appendix: C for activation energy calculation.

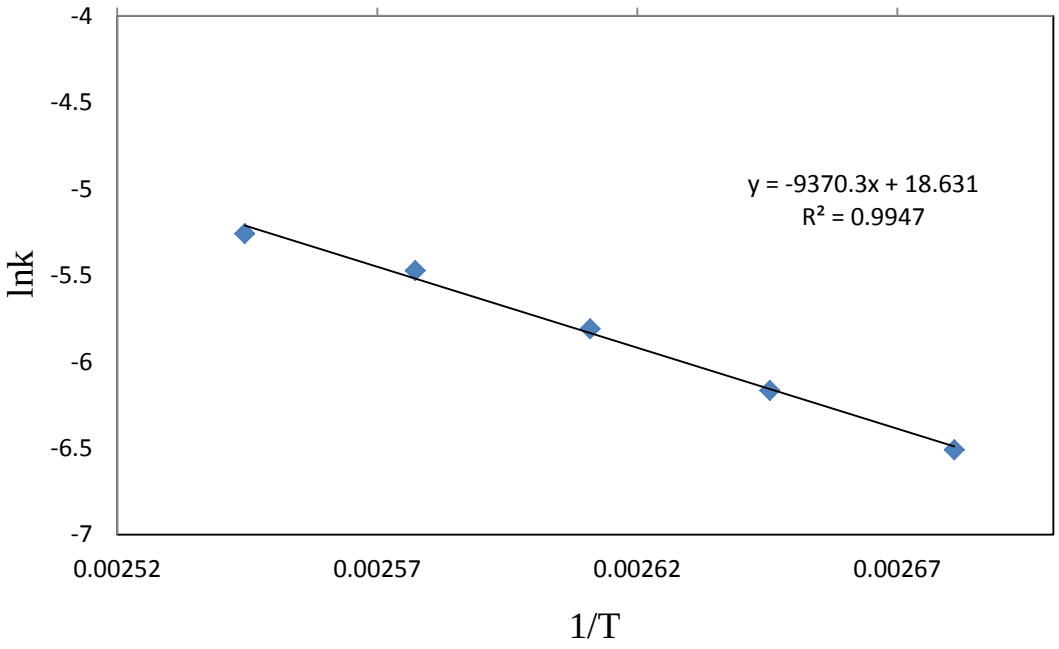

Figure 4.22: Arrhenius plot

The activation energy of 78 kJ/mol signifies that the etherification of glycerol with tert-butanol reaction using $Cs_{2.2}H_{0.8}PW_{12}O_{40}$ supported on SBA-15 catalyst is kinetically controlled. The activation energy is comparable with that ($70\ kJ/mol$) as obtained by Frusteri et al, 2009.

CHAPTER – 5

CONCLUSIONS AND RECOMMENDATIONS

Conclusions

The chemical modification of glycerol with an alcohol can produce glycerol ether. These are the replacements for petroleum derived fuel additives. So this process can increase the glycerol market which is economical to the biodiesel industries. The objective of this work was to develop a catalyst for the effective utilization of glycerol by converting to glycerol ethers. The conclusions obtained from this work are summarized below.

Phase I: Synthesis of catalyst

- Etherification of glycerol with tert-butanol can effectively take place in the presence of solid acid catalyst. The required catalyst was prepared with the impregnation of heteropolyacids on porous support, because heteropolyacids were highly acidic in nature, its presence can enhanced the number and acidic strength of the acidic sites on support.
- SBA-15 was chosen for its higher pore volume, which was prepared using hydrothermal method. Heteropolyacids were incorporated on the support using wetness incipient method.
- The catalyst samples were characterized and the decrease in textural properties (surface area and pore volume) was observed after impregnation. The Keggin structure was formed on SBA-15 by HPA for Cs loading between 2.2 and 2.9. The change in crystal structure was observed with wide angle XRD, structural

morphology was found with SEM. The catalyst with composition of $Cs_{2.2}H_{2.2}PW_{12}O_{40}$ was screened and used in phase-II.

Phase II: Optimization of process parameters and kinetic study

- The process was studied for the effect of temperature, catalyst loading, molar ratio (glycerol/TBA) and found that the increase in temperature has significant effects on glycerol conversion and mono tert-butyl glycerol ether yield. Maximum glycerol conversion of 76% was achieved at the conditions of 120 ˚C, 1 MPa, 1:5 molar ratio (glycerol/TBA), 3% (w/v) catalyst loading, 800 rpm and 5 h.
- The catalyst re-usability study was performed at the optimized condition. The changes in glycerol conversion from 76 % to 73 % during third run signifying that the catalyst is stable at the reaction conditions.
- Reaction was endothermic and followed second order kinetics. The mathematical rate expression was derived based on Langmuir-Hinshelwood mechanism.
- The derived model was fitting for the temperature range of 100 – 120 °C and the activation energy of 78 kJ/mol shows that the reaction was kinetically controlled.

Recommendations

For the production of oxygenated fuel additive from glycerol etherification with tert-butanol, the following recommendations are put forth for future studies.

- The catalyst can produce mono, di and tri tert-butyl glycerol ethers, but it is difficult to produce single ether during etherification process. For the separation of ethers molecular distillation may be required to obtain pure products.
- The optimized catalyst consists of 0.99 cc/g of pore volume. Hence, it can accommodate further loading of heteropolyacids (HPA). The increase in HPA loading can help to increase the glycerol conversion.
- Laboratory scale study on the influence of glycerol ether on diesel/biodiesel performance as well as economic evaluation should be done to conclude if this process is viable.

CHAPTER – 6

REFERENCES

Adhikari S., S D. Fernando and A. Haryanto, "Hydrogen production from glycerin by steam reforming over nickel catalysts," Renew. Energ. **33**, 1097 – 1100 (2008).

Alaya, M. N., B. S. Girgis and W. E. Mourad, "Activated carbon from some agricultural wastes under action of one step steam pyrolysis," J. Porous Mat. **7**, 509-517 (2000).

Atia H., U. Armbruster and A. Martin, "Dehydration of glycerol in gas phase using heteropolyacid catalysts as active compounds," J. Catal. **258**, 71–82 (2008).

Azargohar R. and A. K. Dalai, "Steam and KOH activation of biochar: Experimental and modeling studies," Micropor. Mesopor. Mat. **110**, 413–421 (2008).

Behr A., J. Eilting, K. Irawadi, J. Leschinski and F. Linder, "Improved utilisation of renewable resources: New important derivatives of glycerol," Green Chem. **10**, 13 – 30 (2008).

Boahene P. E., K. K. Soni, A. K. Dalai and J. Adjaye, "Application of different pore diameter SBA-15 supports for heavy gas oil hydrotreatment using FeW catalyst," Appl. Catal. A: Gen. **402**, 31-40 (2011).

Bokade V. V. and G. D. Yadav, "Dodecatungstophosphoric acid supported on acidic clay catalyst for disproportionation of ethylbenzene in the presence of C8 aromatics," Ind. Eng. Chem. Res. **51**, 1209–1217 (2012).

Brandner A., K. Lehnert, A. Bienholz, M. Lucas and P. Claus, "Production of biomass-derived chemicals and energy: Chemocatalytic conversions of glycerol," Top Catal. **52**, 278-287 (2009).

Carraretto C., A. Macor, A. Mirandola, A. Stoppato and S. Tonon, "Biodiesel as alternative fuel: Experimental analysis and energetic evaluations," Energy **29**, 2195-2211 (2004).

Chang A. F. and Y. A. Liu, "Integrated process modeling and product design of biodiesel manufacturing," Ind. Eng. Chem. Res. **49**, 1197–1213 (2010).

Cheng C. K., S. Y. Foo and A. A. Adesina, "Thermodynamic analysis of glycerol-steam reforming in the presence of CO_2 or H_2 as carbon gasifying agent," Int. J. Hydrogen Energ. **37** (2012)

Chetpattananondh P., and C. Tongurai, "Synthesis of high purity monoglycerides from crude glycerol and palm stearin," Songklanakarin J. Sci. Technol. **30** (4), 515-521 (2008).

Ciftci A., B. Peng, A. Jentys, J. A. Lercher, E. J. M. Hensen, "Support effects in the aqueous phase reforming of glycerol over supported platinum catalysts," Appl. Cat. A: Gen. **431– 432**, 113– 119 (2012).

Clacens J. M., Y. Pouilloux and J. Barrault, "Selective etherification of glycerol to polyglycerols over impregnated basic MCM-41 type mesoporous catalysts," Appl. Catal. A: Gen. **227**, 181-190 (2002).

Coulson J. M., J. F. Richarson, "Chemical Engineering," 2nd edition, Pergamon Press (1976).

Da Silva C. R. B., V. L. C. Gonclaves, E. R. Lachter and C. J. A. Mota, "Etherification of glycerol with benzyl alcohol catalyzed by solid Acids," J. Brazilian Chem. Soc. **20:2**, 201-204 (2009).

Dasari M. A., P. P. Kiatsimkul, W. R. Sutterlin and G. J. Suppes, "Low-pressure hydrogenolysis of glycerol to propylene glycol," Appl. Catal. A: Gen. **281** (1-2), 225-231 (2005).

Davda R. R., J. W. Shabaker, G. W. Huber, R, D. Cortright and J. A. Dumesic, "A review of catalytic issues and process conditions for renewable hydrogen and alkanes by aqueous-phase reforming of oxygenated hydrocarbons over supported metal catalysts," Appl. Catal. B: Environ. **56,** 171-186 (2005).

Demirbas A., "Progress and recent trends in biofuels. Process Energy Combustion," Sci. **33**, 1-18 (2007).

Demirel S., K. Lehnert, M. Lucas and P. Claus, "Use of renewable for the production of chemicals: Glycerol oxidation over carbon supported gold catalysts," Appl. Catal. B: Environ. **70**, 637-643 (2007).

Dorado M. P., E. Ballesteros, J.M. Arnal, J. Gomez and F.J. Lopez," Exhaust emissions from a Diesel engine fueled with transesterified waste olive oil," Fuel **82,** 1311–1315 (2003).

www.enotes.com/public-health-encyclopedia/fuel-additives March 10th, 2011

Fan X., R. Burton and Y. Zhou, "Glycerol (byproduct of biodiesel production) as a source for fuels and chemicals – mini review," The Open Fuels and Energy Science **3**, 17 – 22 (2010).

Fernandez Y., A. Arenillas, J. M. Bermudez and J. A. Menendez, "Comparative study of conventional and microwave-assisted pyrolysis, steam and dry reforming of glycerol for syngas production, using a carbonaceous catalys," J. Anal. Appl. Phys. **88**, 155-159 (2010).

Fogler H. S., “Elements of chemical reaction engineering,” 3rd edition, Prentice-Hall of India Private Limited (2004).

Frusteri F., F. Arena, G. Bonura, C. Cannilla, L. Spadaro and O. Di Blasi, “Catalytic etherification of glycerol by tert-butyl alcohol to produce oxygenated additives for diesel fuel,” Appl. Catal. A: Gen. **367**, 77-83 (2009).

Gu Y., A. Azzouzi, Y. Pouilloux, F. Jerome and J. Barrault, “Heterogeneously catalyzed etherification of glycerol: new pathways for transformation of glycerol to more valuable chemicals,” Green Chem. **10**, 164-167 (2008).

Guerrero-Perez M. O., J. M. Rosas, J. Bedia, J. R. Mirasol and T. Cordero, “Recent inventions in glycerol transformations and processing,” Recent Pat. Chem. Eng. **2**, 11-21 (2009).

Hermida L., A. Z. Abdullah and A. R. Mohamed, “Synthesis of monoglyceride through glycerol esterification with lauric acid over propyl sulfonic acid post-synthesis functionalized SBA-15 mesoporous catalyst,” Chem. Eng. J. **174**, 668– 676 (2011).

Hong, A. A., K. K. Cheng, F. Peng, S. Zhou, Y. Sun, C. M. Liu and D. H. Liu, “Strain isolation and optimization of process parameters for bioconversion of glycerol to lactic acid,” J. of Chem. Tech. Biotech. **84**, 1576-1581 (2009).

Iaonnidou O. and A. Zabaniotou, “Agricultural residues as precursors for activated carbon production – A review,” Renew. Sus. Energ. Rev. **11**, 1966-2055 (2007).

Jamroz M. E., M. Jarosz, J. Witowska-Jarosz, E. Bednarek, W. Tecza, M. H. Jamroz, J. C. Dobrowolski and J. Kijenski, “Mono-, di-, and tri-tert-butyl ethers of glycerol: A molecular spectroscopic study,” Spectrochimi. Acta Part A **67**, 980-988 (2007).

Janaun J. and N. Ellis, “Perspectives on biodiesel as a sustainable fuel,” Renew. Sust. Energ. Rev. **14**, 1312–1320 (2010).

Johnson D. T., and K. A. Taconi, “The Glycerin Glut: Options for the value-added conversion of crude glycerol resulting from biodiesel production,” Environ. Prog. **26:4**, 338-348 (2007).

Kapil Dev Pathak, Catalytic conversions of glycerol to value added liquid chemicals, Master’s thesis, University of Saskatchewan (2005).

Karinen R. S and A. O. I. Krause, “New biocomponents from glycerol,” Appl. Cat. A: Gen. **306**, 128 – 133, (2006).

Khamduang M., K. Packdibamrung, J. Chutmanop, Y. Chisti and P. Srinophakun, “Production of L-phenylalanine from glycerol by a recombinant Escherichia coli,” J. Ind. Microbiol. Biot. **36,** 1267-1274 (2009).

Kiatkittipong W., P. Intaracharoen, N. Laosiripojana, C. Chaisuk, P. Praserthdam and S. Assabumrungrat, “Glycerol ethers synthesis from glycerol etherification with tert-butyl alcohol in reactive distillation,” Computers and Chemical Engineering **35**, 2034– 2043 (2011).

Klepacova K., D. Mravec, E. Hajekova and M. Bajus, “Etherification of glycerol,” Petroleum and Coal, **45**, 1-2, 54-57 (2003).

Klepacova K., D. Mravec, A. Kaszonyi and M. Bajus, “Etherification of glycerol and ethylene glycol by isobutylene,” Appl. Catal. A: Gen. **328**, 1-13 (2007).

Lapuerta M., O. Armas, J. R. Fernandez, “Effect of biodiesel fuels on diesel engine emissions,” Prog. Energ. Combust. **34**, 198–223 (2008).

Lee H J., D. Seung, K. S. Jung, H. Kim and I. N. Filimonov, "Etherification of glycerol by isobutylene: Tuning the product composition," Appl. Catal. A: Gen. **390**, 235-244 (2010).

Lee S., D. Posarac and N. Ellis, "Process simulation and economic analysis of biodiesel production processes using fresh and waste vegetable oil and supercritical methanol," Chem. Eng. Res. Des. **89**, 2626–2642 (2011).

Lehmann J., M. C. Rillig, J. Thies, C. A. Masiello, W. C. Hockaday and D. Crowley, "Biochar effects on soil biota- A review," Soil Biol. Biochem. **43**, 1812-1836 (2011).

Lua, A. C., T. Yang and J. Guo, "Effects of pyrolysis conditions on the properties of activated carbons prepared from pistachio-nutshells," J. Anal. Appl. Pyrol., **72**, 279-287 (2004).

Luković N., Z. Knežević-Jugović and D. Bezbradica, "Biodiesel Fuel Production by Enzymatic Transesterification of Oils: Recent Trends," Challenges and Future Perspectives, Alternative Fuel.

Ma F. and M. A. Hanna, "Biodiesel Production: A Review," Bio Res. Tech. **70 (1)**, 1-15 (1999).

Maggio G and G. Cacciola, "When will oil, natural gas, and coal peak?," Fuel **98**,111–123 (2012).

Mao Z. B., T. L. Luo, H. T. Cheng, M. Liang, and G. J. Liu, "Intrinsic kinetics of catalytic hydrogenation of cardanol," Ind. Eng. Chem. Res., **48**, 9910–9914 (2009).

Meher L. C., R. Gopinath, S. N. Naik and A. K. Dalai, "Catalytic hydrogenolysis of glycerol to propylene glycol over mixed oxides derived from a hydrotalcite-type precursor," Ind. Eng. Chem. Res. **48**, 1840-1846 (2009).

Melero J. A., G. Vicente, G. Morales, M. Paniagua, J. M. Moreno, R. Roldan, A. Ezquerro and C. Perez, "Acid-catalyzed etherification of bio-glycerol and isobutylene over sulfonic mesostructured silicas," Appl. Catal. A: Gen. **346**, 44-51 (2008).

Narasimharao K., D.R. Brown, A.F. Lee, A.D. Newman, P.F. Siril, S.J. Tavener and K. Wilson, "Structure–activity relations in Cs-doped heteropolyacid catalysts for biodiesel production," J. Catal. **248**, 226–234 (2007).

Ni J., J. J. Pignatello and B. Xing, "Adsorption of Aromatic Carboxylate Ions to Black Carbon (Biochar) Is Accompanied by Proton Exchange with Water," Environ. Sci. Technol. **45**, 9240–9248 (2011).

Noureddini H., W. R. Dailey and B. A. Hunt, "Proudction of ethers of glycerol from crude glycerol – the byproduct of biodiesel production" University of Nebraska – Lincoln Available at http://digitalcommons.unl.edu/cgi/viewcontent.cgi?article=1019&context=chemeng_ biomaterials (1998) (5th July, 2012)

Oberweis S and T.T Al-Shemmeri, "Effect of biodiesel blending on emissions and efficiency in a stationary diesel engine," International Conference on Renewable Energies and Power Quality (ICREPQ'10) Granada (Spain), 23th to 25th March (2010).

Olga Guerrero-Perez M., J. M. Rosas, J. Bedia, J. R. Mirasol and T. Cordero, "Recent inventions in glycerol transformations and processing," Recent pat. Chem. Eng. **2**, 11-21 (2009).

Pachauri N. and B. He, "Value-added utilization of crude glycerol from biodiesel production: A survey of current research activities," An ASABE Meeting Presentation (2006).

Park S., D. R. Park, J. H. Choi, T. J. Kim, Y. M. Chung, S. H. Oh and I. K. Songa, "Direct synthesis of hydrogen peroxide from hydrogen and oxygen over insoluble Cs2.5H0.5PW12O40 heteropolyacid supported on Pd/MCF," J. Mol. Cat. A: Chem. **332**, 76–83 (2010).

Prabhu N., A.K. Dalai and J. Adjaye, "Hydrodesulphurization and hydrodenitrogenation of light gas oil using NiMo catalyst supported on functionalized mesoporous carbon," Appl. Catal. A: Gen. **401**, 1-11 (2011).

Qadeer, R., J. Hanif, , M. A. Saleem And M. Afzal, "Characterization of activated charcoal," J. of the Chem. Soc. Pakistan, **16**, 229-235 (1994).

Quigley R. and Robert H. Barbour, "Biodiesel quality improvement with additive treatment," SAE Fuels & Lubricants Meeting & Exhibition, June 2004.

Quintana N. and F. V. der Kooy, M. D. Van de Rhee and G. P. Voshol, "Renewable energy from Cyanobacteria: energy production optimization by metabolic pathway engineering," Appl. Microbiol. Biotechnol. **91**, 471–490 (2011).

Qurashi M. M. and E. T. Hussain, 2005 "Renewable Energy Technologies for Developing Countries Now and to 2023,"

Ramachandran, P.A. and R.V. Chaudhari, "Three phase catalytic reactors," Gordon and Breach Science, Paris (1983).

Rattanaphra D., A. P. Harvey, A. Thanapimmetha and P. Srinophakun, "Simultaneous transesterification and esterification for biodiesel production with and without a sulphated zirconia catalyst," Fuel **97** 467–475 (2012).

Ringer M., V. Putsche and J. Scahill, "Large-Scale Pyrolysis Oil Production: A Technology Assessment and Economic Laboratory," NREL/TP-510-37779, (2006).

Rodriquez-Reinoso, F. and M. Molina-Sabio, "Activated carbons from Lignocellulosic materials by chemical and/or physical activation: An overview," Carbon **30** (7), 1111-1118 (1992).

Ruppert A. M., J. D. Meeldijk, B. W. M. Kuipers, B. H. Erne and B. M. Weckhuysen, "Glycerol Etherification over Highly Active CaO-based materials: New mechanistic aspects and related colloidal particle formation," Chemistry A European J. **14**, 2016-2024 (2008).

Rymowicz, W., A. Rywinska, B. Zarowska and P. Juszczyk, "Citric acid production from raw glycerol by acetate mutants of Yarrowia lipolytica," Chem. Pap. **60** (5), 391-394 (2006).

Satterfield C. N, Heterogeneous Catalysis in Industrial Practice, 2nd edition, McGraw-Hill, New York, (1991).

Singh A. K and S. D. Fernando, "Preparation and Reaction Kinetics Studies of Na-based Mixed Metal Oxide for Transesterification," Energy Fuels **23**, 5160–5164, (2009).

Song C, "Global challenges and strategies for control, conversion and utilization of CO2 for sustainable development involving energy, catalysis, adsorption and chemical processing," Catal. Today **115**, 2–32 (2006).

Soni K., P.E. Boahene, K. Chandra Mouli, A.K. Dalai and J. Adjaye, "Hydrotreating of coker light gas oil on Ti-HMS supported heteropolytungstic acid catalysts," Appl. Catal. A: Gen. **398**, 27–36 (2011).

Tisserat B., R. H. O'kuru, H. Hwang, A. A. Mohamed, R. Holser, "Glycerol Citrate Polyesters Produced Through Heating Without Catalysis," J. Appl. Polym. Sci. **125**, 3429-3437 (2012).

Valliyappan T., N. N. Bakshi and A. K. Dalai, "Hydrolysis of glycerol for the production of hydrogen or syn gas," Bioresource Technol. **99**, 4476-4483 (2008).

Valliyappan T., D. Ferdous, N. N. Bakshi and A. K. Dalai, "Production of hydrogen and syngas via steam gasification of glycerol in a fixed-bed reactor," Top Catal. **49**, 59-67 (2008).

Veldsink J. W., G. F. Versteeg, W. P. M. van Swaaij, "Intrinsic kinetics of the oxidation of methane over an industrial copper (II) oxide catalyst on γ-alumina support," Chem. Eng. J. **57**, 273-283 (1995).

Vinu, A., P. Srinivasu, M. Miyahara, and K. Ariga, "Preparation and Catalytic Performances of Ultra large – Pore TisBA – 15 Mesoporous Molecular Sieves with Very High Ti Content," J. Phys. Chem. B **110**, 801 – 806 (2006).

Watanabe M., T. Iida, Y. Aizawa, T. M. Aida and H. Inomata, "Acrolein synthesis from glycerol in hot-compressed water," Bioresource Technol. **98**, 1285–1290, (2007).

Wilke C. R and Chang P, "Correlation of diffusion coefficients in dilute solutions," A1ChE. Journal, **1** (2), 264 - 269 (1955).

Wolfson A., and C. Dlugy, "Glycerol as an alternative green medium for carbonyl compound reductions," Org. Comm. **2:2**, 34-41 (2009).

Wright M. M., R. C. Brown and A. A. Boateng, "Distributed processing of biomass to bio-oil for subsequent production of Fischer-Tropsch liquids," Biofuels Bioprod. Bioref. **2**, 834-843 (2008).

Xiao L., J. Mao, J. Zhou, X. Guo and S. Zhang, "Enhanced performance of HY zeolites by acid wash for glycerol etherification with isobutene," Appl. Catal. A: Gen. **393**, 88–95 (2011).

Yadav G. D., G. George, “Single step synthesis of 4-hydroxybenzophenone via esterification of and fries rearragement: Novelty of Cesium heteropoly acid on clay,” J. Mol. Cat. A: Chem. **292**, 54-61 (2008).

Yadav G. D., P. A. Chandan and N.Gopalaswami, “Green etherification of bioglycerol with 1-phenyl ethanol over supported heteropoly acid,” Clean Technol. Envir. **14** (1), 85-95 (2012).

Yazdani S. S., and R. Gonzalez, “Anaerobic fermentation of glycerol: a path to economic viability for the biofuels industry,” Curr. Opin. Biotech. **18**, 213-219 (2007).

Yoshikawa T., M. Mukaida, T. Tago and T. Masuda, “Production of valuable chemicals from glycerol over Zirconia-iron oxide composite catalyst,” Division of Chemical System Engineering, Hokkaido University, Japan

Zhang T., W. P. Walawender, L. T. Fan, M. Fan, D. Daugaard and R. C. Brown, “Preparation of activated carbon from forest and agricultural residues through CO2 activation,” Chem. Eng. J. **105**, 53-59 (2004).

Zhao W., B. Yang, C. Yi, Z. Lei and J. Xu, “Etherification of glycerol with isobutylene to produce oxygenate additive using sulfonated peanut shell catalyst,” Ind. Eng. Chem. Res. **49**, 12399–12404 (2010).

Zieba A., L. Matachowski, E. Lalik and A. Drelinkiewicz, “Methanolysis of Castor Oil Catalysed by Solid Potassium and Cesium Salts of 12-Tungstophosphoric Acid,” Catal. Lett. **127**, 183–194 (2009).

Appendix: A Calculation of effectiveness factor for the internal mass transfer resistance study

The effectiveness factor (η) is defined as the ratio of actual overall rate of reaction to the rate of reaction that would result if entire interior surface were exposed to the external pellet surface conditions (Fogler, 2004).

The diffusional limitation can be determined from Thiele modulus (Φ) and effectiveness factor.

$\Phi > 3$ and $\eta < 0.3 \rightarrow$ Internal diffusion limits the reaction

$\Phi < 3$ and $\eta > 0.7 \rightarrow$ Surface reaction limits the reaction

The effectiveness factor (η) is determined by

$$\eta = \frac{3}{\Phi^2}\{\Phi \coth \Phi - 1\} \quad \text{(A. 1) (Fogler, 2004)}$$

The Thiele modulus (Φ) is given by

$$\Phi^2 = \frac{k_n \rho_e S_a C_{AS}^{n-1} R^2}{D_e} \quad \text{(A. 2) (Fogler, 2004)}$$

k_n - Rate constant

ρ_e – Density of the catalyst

S_a – Surface area

C_{AS} - Concentration of A at catalyst surface

R – Radius of catalyst particle

D_e – Effective diffusivity

The effective diffusivity can be measured by passing two fluids past opposite faces of catalyst pellet and measuring the flux of one fluid to other (Satterfield, 1991). In glycerol and tert-butanol mixture, glycerol is assumed to diffuse in to tert-butanol.

The effective diffusivity is given by

$$D_e = \frac{D_{AB}\,\varphi\,\sigma}{\xi} \quad \text{(A. 3)(Fogler, 2004)}$$

D_{AB} - Diffusion co-efficient of glycerol in tert-butanol

φ - Pellet porosity

Porosity or void fraction is defined as the fraction of the volume of the particle which is not occupied by solid material (Coulson and Richarson, 1976).

ξ - Tortuosity = 3 (Yadav et al., 2012)

σ - Constriction factor = 1 (uniform pore area)

Diffusion in liquid phase can be calculated using Wilke – Chang equation.

$$D_{AB} = \frac{7.4 * 10^{-8} * (\psi M_B)^{0.5}\, T}{\mu * (v_a)^{0.6}} \quad \text{(A. 4)(Wilke and Chang, 1955)}$$

ψ – Association factor of glycerol = 1 (Yadav et al., 2012)

μ - Tert-butanol viscosity = 3.35 cP

v_a - Molar volume of glycerol

$$v_a = \frac{92\ \text{g/mol}}{1.261\ \text{g/cm}^3}$$

$$v_a = 73\ \text{cm}^3/\text{mol}$$

$$D_{AB} = \frac{7.4 * 10^{-8} * (74)^{0.5}\, 393}{3.35 * (73 * 10^{-6})^{0.6}}$$

$$D_{AB} = 5.7 * 10^{-6}\ \text{cm}^2/\text{s} = 5.7 * 10^{-10}\ \text{m}^2/\text{s}$$

Substitution of D_{AB}, φ and ξ values in equation (A.3)

$$D_e = \frac{5.7 * 10^{-10} * 1 * 1}{3}$$

$$D_e = 1.9 * 10^{-10}\ \text{m}^2/\text{s}$$

Substitution of effective diffusivity (D_e) in equation (A.2)

$$\Phi^2 = \frac{0.0052 * 126 * 707 * 1.9 * (2.46 * 10^{-9})^2}{1.133 * 10^{-14}}$$

$$\Phi = 0.686$$

Substitution of Thiele modulus (Φ) in equation (A.1)

$$\eta = \frac{3}{(0.686)^2} \{0.686 \coth(0.686) - 1\}$$

$$\eta = 0.972$$

From the above calculations, it is observed that the Thiele modulus is less than 3 and effectiveness factor is greater than 0.7, therefore internal diffusional resistance is negligible.

Appendix: B Derivation of mathematical expression using Langmuir-Hinshelwood kinetics

The optimized results are used to develop a kinetic model for etherification of glycerol. In this reaction, glycerol (G) and TBA (T) react to produce MTBGE (M) and water (W) as products. According to Langmuir-Hinshelwood kinetics, the reaction is controlled by 3 steps, viz. adsorption, surface reaction and desorption (Fogler, 2004).

Step: 1a Adsorption of glycerol is written as

$$G + S \underset{k_{-1}}{\overset{k_1}{\rightleftharpoons}} G.S$$

$$-r_{Ad1a} = k_1 C_G\, C_V - k_{-1} C_{G.S} = 0 \quad ---------- (B.1)$$

$$C_{G.S} = K_1 C_G\, C_V \quad ---------- (B.2)$$

Step: 1b Adsorption of TBA is written as

$$T + S \underset{k_{-2}}{\overset{k_2}{\rightleftharpoons}} T.S$$

$$-r_{Ad1b} = k_2 C_T\, C_V - k_{-2}\, C_{T.S} = 0 \quad ---------- (B.3)$$

$$C_{T.S} = K_2\, C_T\, C_V \quad ---------- (B.4)$$

Step: 2 Surface reaction of the G.S and T.S leads to form MTBGE (M.S) and water (W.S) on the vacant site.

$$G.S + T.S \underset{k_{-3}}{\overset{k_3}{\rightleftharpoons}} M.S + W.S$$

$$-r_S = k_3 C_{G.S}\, C_{T.S} - k_{-3} C_{M.S}\, C_{W.S} \quad ---------- (B.5)$$

Step: 3 Desorption of M.S and W.S is written as

$$M.S \underset{k_{-4}}{\overset{k_4}{\rightleftharpoons}} M + S$$

$$-r_{De1} = k_4 C_{M.S} - k_{-4} C_M C_V = 0 \quad ---------(B.6)$$

$$C_{M.S} = \frac{C_M C_V}{K_4} \quad ----------(B.7)$$

$$W.S \underset{k_{-5}}{\overset{k_5}{\rightleftharpoons}} W + S$$

$$-r_{De2} = k_5 C_{W.S} - k_{-5} C_W C_V = 0 \quad ---------(B.8)$$

$$C_{W.S} = \frac{C_W C_V}{K_5} \quad ----------(B.9)$$

The total concentration of the sites is written as the summation of occupied and vacant sites.

Total sites = (Occupied sites) + (Vacant sites)

$$C_{t,s} = (C_{G.S} + C_{T.S} + C_{M.S} + C_{W.S}) + (C_V) \quad ------(B.10)$$

$$C_{t,s} = C_V + K_1 C_G C_V + K_2 C_T C_V + \frac{C_M C_V}{K_4} + \frac{C_W C_V}{K_5} \quad ------(B.11)$$

$$C_{t,s} = C_V \left(1 + K_1 C_G + K_2 C_T + \frac{C_M}{K_4} + \frac{C_W}{K_5}\right) ------(B.12)$$

The concentration of the vacant site is written as

$$C_V = C_{t,s} \Big/ \left(1 + K_1 C_G + K_2 C_T + \frac{C_M}{K_4} + \frac{C_W}{K_5}\right) ------(B.13)$$

The reaction is controlled by surface reaction (see Appendix: A), so which is taken as slowest step to determine the rate of reaction. Therefore, the equations (B.2), (B.4), (B.7) and (B.9) are substituted in equation (B.5).

$$-r_S = k_3(C_{G.S}\, C_{T.S} - \frac{k_{-3}}{k_3} C_{M.S}\, C_{W.S}) \quad ------(B.14)$$

$$-r_S = k_3 K_1 K_2 (C_G\, C_T (C_V)^2 - \frac{C_M\, C_W\, (C_V)^2}{K_1 K_2\, K_3\, K_4\, K_5}) \quad ------(B.15)$$

$$K_e = K_1 K_2\, K_3\, K_4\, K_5$$

$$-r_S = k_3 K_1 K_2 (C_V)^2 (C_G\, C_T - \frac{C_M\, C_W}{K_e}) ----- (B.16)$$

The value C_V from equation (B.13) is substituted in equation (B.16),

$$-r_S = k_3 K_1 K_2 \left(C_{t,s}/(\,1 + K_1 C_G + \, K_2\, C_T + \frac{C_M}{K_4} + \frac{C_W}{K_5}\,)\right)^2 (C_G\, C_T - \frac{C_M\, C_W}{K_e}\,)\,)(B.17)$$

But, glycerol etherification reactions is reversible (Klepacova et al., 2003), so the above is written as

$$-r_S = K_1 K_2\, k_3 C_G\, C_T \left(C_{t,s}/\left(\, 1 \, + K_1 C_G + \, K_2\, C_T + \frac{C_M}{K_4} + \, \frac{C_W}{K_5}\,\right)\right)^2 --- (B.18)$$

The adsorption and desorption of the species are very weak and values of equilibrium constants are negligible then the above equation is written as

$$-r_S = K_1 K_2\, k_3 C_G\, C_T \left(C_{t,s}\right)^2 \quad ---------(B.19)$$

Total number of the active sites is directly proportional to amount of catalyst loading

$$C_{t,s} = \, k_t w_t$$

k_t= constant

w_t = catalyst loading

$$-r_S = K_1K_2\, k_3C_G\, C_T(k_t\, w_t)^2 \quad -------- (B.20)$$

$$-r_S = K_1K_2\, k_3\, k_t{}^2\, C_G\, C_T(w_t)^2 \quad -------- (B.21)$$

$K_1K_2\, k_3\, k_t{}^2 = k =$ Apparent rate constant

$$-r_S = \; k\, w_t{}^2\, C_G\, C_T \quad ---------- (B.22)$$

$$-r_S = C_{G0}\frac{dX_G}{dt} = \; k\, w_t{}^2\, C_G\, C_T \quad ----- (B.23)$$

C_{G0} and C_{T0} are the initial concentrations of glycerol and tert-butanol.

Let $M = \frac{C_{T0}}{C_{G0}}$ = the initial molar ratio of reactants

C_G and C_T are the concentrations of glycerol and tert-butanol at any time t.

Amount of glycerol reacted = $C_{G0}\, X_G$

Amount of tert-butanol reacted = $C_{T0}\, X_T$

The amounts of glycerol and tert-butanol which have reacted at any time t are equal and given by

$$C_{G0}\, X_G = \; C_{T0}\, X_T \quad ---------- (B.24)$$

$$C_G = C_{G0}(1 - \; X_G) \quad ---------- (B.25)$$

$$C_T = C_{T0}(1 - \; X_T) \quad ---------- (B.26)$$

By rearranging the above equation we can get

$$C_T = C_{T0} - C_{T0} X_T \quad ----------(B.27)$$

$$C_T = M C_{G0} - C_{G0} X_G \quad ----------(B.28)$$

Substituting (B.25) and (B.28) in (B.23), we can get

$$C_{G0} \frac{dX_G}{dt} = k w_t^{\,2} C_{G0}(1 - X_G)(M - X_G) C_{G0} \quad ----------(B.29)$$

$$\frac{dX_G}{dt} = K w_t^{\,2} C_{G0}(1 - X_G)(M - X_G) \quad ----------(B.30)$$

$$\frac{dX_G}{(1 - X_G)(M - X_G)} = k w_t^{\,2} C_{G0}\, dt \quad ----------(B.31)$$

By integrating the above equation in the limits

$$\text{at } t = 0,\ X_G = 0$$

$$\text{at } t = t,\ X_G = X_G$$

$$\int_0^{X_G} \frac{dX_G}{(1 - X_G)(M - X_G)} = K w_t^{\,2} C_{G0} \int_0^t dt \quad ----------(B.32)$$

$$\frac{1}{(M - 1)} \ln \frac{(M - X_G)}{M(1 - X_G)} = K w_t^{\,2} C_{G0}\, t \quad ----------(B.33)$$

By rearranging we can get

$$\ln \frac{(M - X_G)}{M(1 - X_G)} = (M - 1) k w_t^{\,2} C_{G0}\, t, \qquad M \neq 1 \quad ----------(B.34)$$

This is the desired integrated rate equation for second order reaction with $C_{G0} \neq C_{T0}$ in terms of conversion.

Appendix: C Calculation of activation energy using Arrhenius equation

The Arrhenius equation is written as

$$k = k_0 \exp(-E/RT) - - - - - - - - - - - - - (C.1)$$

$k_0 \rightarrow$ Frequency factor

$E \rightarrow$ Activation Energy

$R \rightarrow$ Gas constant

$T \rightarrow$ Temperature

$$\ln k = \ln k_0 - E/RT - - - - - - - - - - - - - - - (C.2)$$

Rate constant at different temperatures was shown in Table 4.7

lnk plotted against with 1/T (see Figure 4.22).

From the Figure 4.22, the slope of the line is written as

$$\text{slope} = \frac{-E}{R} = -9370.3$$

$$E = 9370.3 * 1.9872 \text{ Cal mol}^{-1}$$

$$E = 18{,}621 \text{ Cal mol}^{-1}$$

$$1 \text{ cal} = 4.184 \text{ joules}$$

$$E = 19{,}356 * 4.184 \text{ J mol}^{-1}$$

$$E = 77{,}910.3 \frac{J}{mol}$$

$$E = 78 \text{ kJ/mol}$$

Therefore, the activation energy for etherification of glycerol with tert-butanol is 78 kJ/mol.

Appendix: D Calculation of activation properties

The Eyring equation is useful to determine the activation parameters such as enthalpy of activation, entropy of activation and Gibb's free energy. From these the temperature dependence of reaction rate and the spontaneity of the reaction can be identified.

The linear form of the Eyring equation is

$$\ln\left(\frac{k}{T}\right) = -\frac{\Delta H^{\ddagger}}{R}\frac{1}{T} + \ln\left(\frac{k_B}{h}\right) + \frac{\Delta S^{\ddagger}}{R} \quad \text{----------(D. 1)}$$

k_B = Boltzmann's constant = $1.381 * 10^{-23}$ J/K

T = absolute temperature in K

h = Plank constant = $6.626 * 10^{-34}$ J s

k = rate constant

R = Universal gas constant = 8.314 J/mol/K

$\Delta H^{\ddagger}$ = activation enthalpy = kJ/mol

$\Delta S^{\ddagger}$ = activation entropy = J/mol/K

The value of $\ln\left(\frac{k}{T}\right)$ (from Table 4.7) is plotted against $\frac{1}{T}$ (see Figure D.1). The activation enthalpy is calculated from the slope of the line.

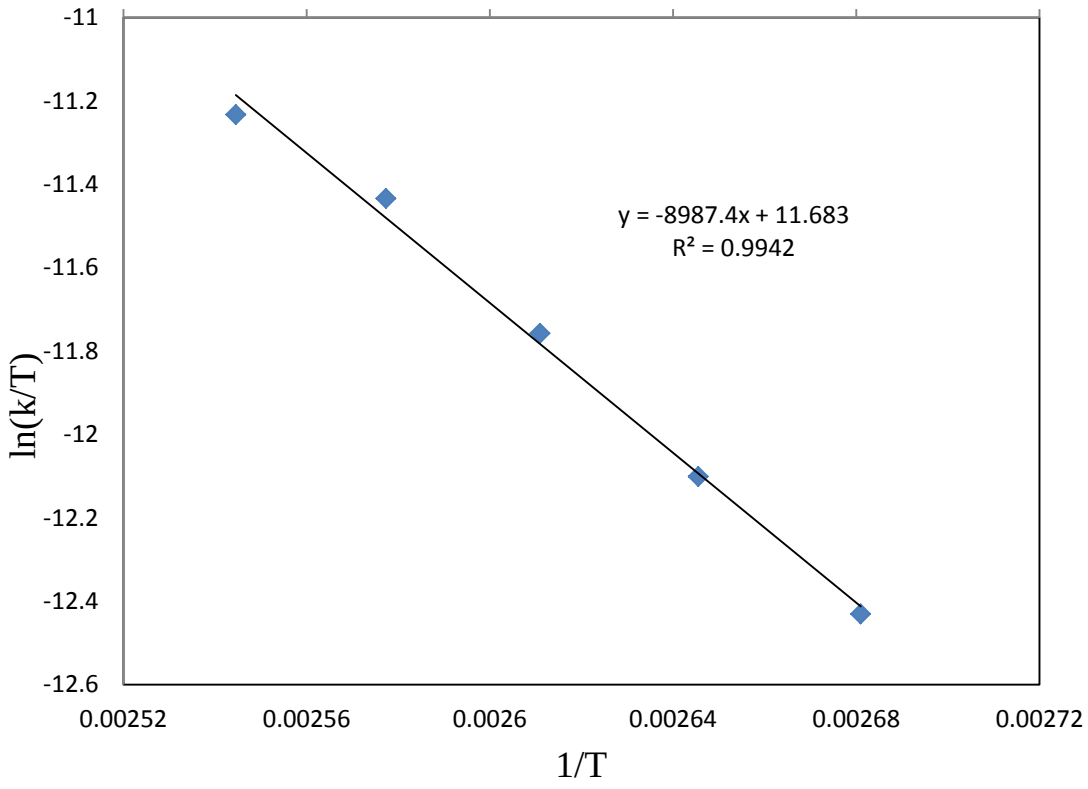

Figure D.1: Eyring plot ($\ln\left(\frac{k}{T}\right)$ against $\frac{1}{T}$)

From the Figure D.1, the slope of the line equal to -8987.4, which is equal to

Slope = $-\frac{\Delta H^{\ddagger}}{R}$ = -8987.4

$\Delta H^{\ddagger}$ = 74.72 kJ/mol

$$\Delta G^{\ddagger} = \Delta H^{\ddagger} - T * \Delta S^{\ddagger} \quad (D.2)$$

$\Delta G^{\ddagger}$ = Gibb's free energy = kJ/mol

$\Delta G^{\ddagger}$ is considered as the driving force of the chemical reaction. $\Delta G^{\ddagger}$ determines the spontaneity of the reaction.

$\Delta G^{\ddagger} < 0 \rightarrow$ reaction is spontaneous

$\Delta G^{\ddagger} = 0 \rightarrow$ system at equilibrium, not net change occurs

$\Delta G^{\ddagger} > 0 \rightarrow$ reaction is not spontaneous

From the Figure D.1, the intercept of the line is 11.683, which is equal to

$$\ln\left(\frac{k_B}{h}\right) + \frac{\Delta S^{\ddagger}}{R} = 11.683$$

$$\ln\left(\frac{1.381 * 10{-}23\ \mathrm{J/K}}{6.626 * 10{-}34\ \mathrm{J\,s}}\right) + \frac{\Delta S^{\ddagger}}{R} = 11.683$$

$$23.76 + \frac{\Delta S^{\ddagger}}{R} = 11.683$$

$\Delta S^{\ddagger}$ = - 100 J/mol/K

From Arrhenius equation

$$k = k_0 \exp(-E/RT) \quad \text{(D. 3)}$$

$$\ln k = \ln k_0 - E/RT \quad \text{(D. 4)}$$

Comparison of Arrhenius equation with Eyring equation

$$E = \Delta H^{\ddagger} + RT \quad \text{(D. 5)}$$

Low values of E and $\Delta H^{\ddagger} \rightarrow$ fast rate

High values of E and $\Delta H^{\ddagger} \rightarrow$ slow rate

The typical values of E and $\Delta H^{\ddagger}$ are in between 20 and 150 kJ/mol.

Activation energy was determined as 78 kJ/mol using Arrhenius equation.

The values of $\Delta H^{\ddagger}$, R and T are substituted in equation (D.5).

$\Delta H^{\ddagger} + RT$ = 74.72 kJ/mol + 8.314 * 393 J/mol

= 74.72 kJ/mol + 3267 J/mol

= 77.987 kJ/mol = 78 kJ/mol

$$\Delta G^{\ddagger} = 74.72 - 393 * (-0.1) = 113.7 \text{ kJ/mol}$$

The etherification of glycerol reaction with tert-butanol is not spontaneous ($\Delta G^{\ddagger}$ = 113.7 kJ/mol).

Appendix: E Mass balance at optimized reaction conditions

The mass balances were performed at the optimized reaction conditions such as 120 °C, 1MPa, 3% catalyst loading, 1:5 molar ratio (glycerol/tert-butanol), 800 rpm and 5 hours

Glycerol conversion = 76%, Selectivities (mono-74, di-20 and tri-6)

Table E.1: Mass balance at optimized reaction conditions

Material	**Input**		**Output**	
	Moles	**Mass(g)**	**Moles**	**Mass(g)**
Glycerol	0.1087	10	0.026	2.4
Tert-butanol	0.5435	40.2	0.35	25.9
Mono ether	-	-	0.062	10.6
Di ether	-	-	0.017	3.8
Tri ether	-	-	0.005	1.6
Water	-	-	0.25	4.5
	(50.2 – 1.2*) = 49.0 g		48.8 g	

Initial mass of the reaction mixture is 50.22 g

*1.2 g of reaction mixture was taken for GC analysis, the rest of the reaction mixture would be 49.02 g

After the reaction, the mass of the products with unreacted reactants was found to be 48.8g.

Therefore, the change in mass of the reaction mixture unaccounted is 0.2 g.

From the mass balance, the reaction volume throughout reaction was found to be constant. Therefore, at any given experimental run, the conversion of glycerol definition such as ratio of change in molar concentration to the initial molar concentration was validated.

Appendix: F Calibration graphs

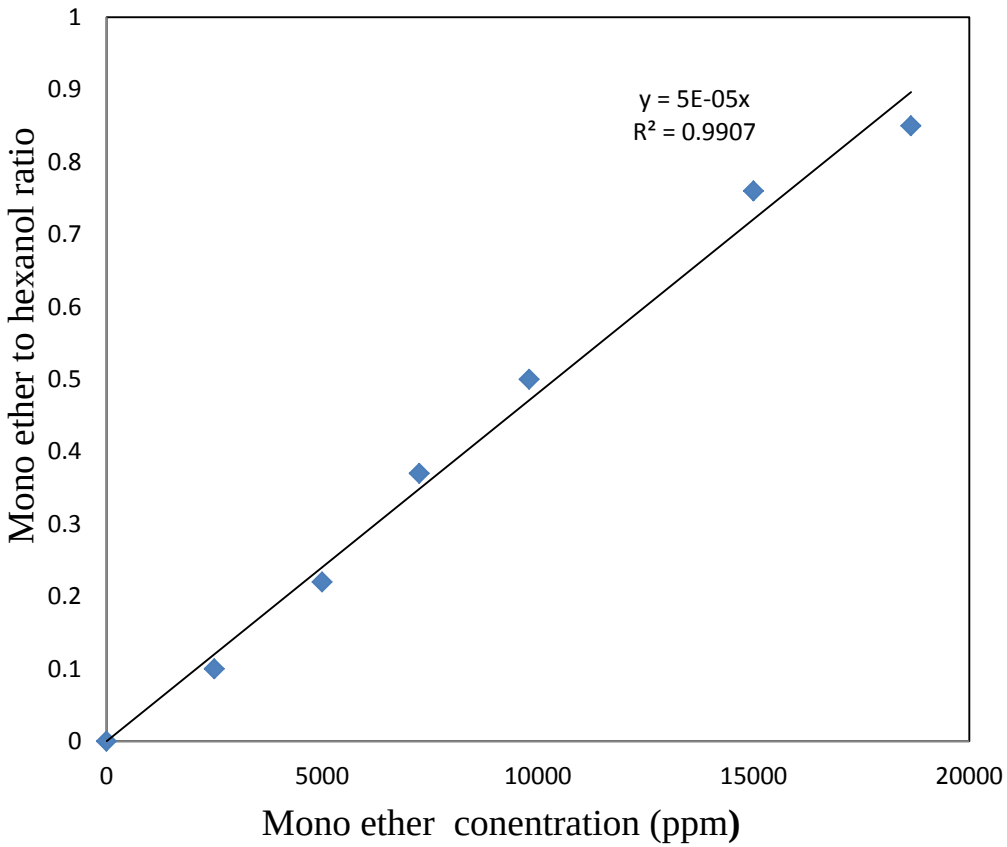

Figure E.1: Mono tert-butyl glycerol ether calibration

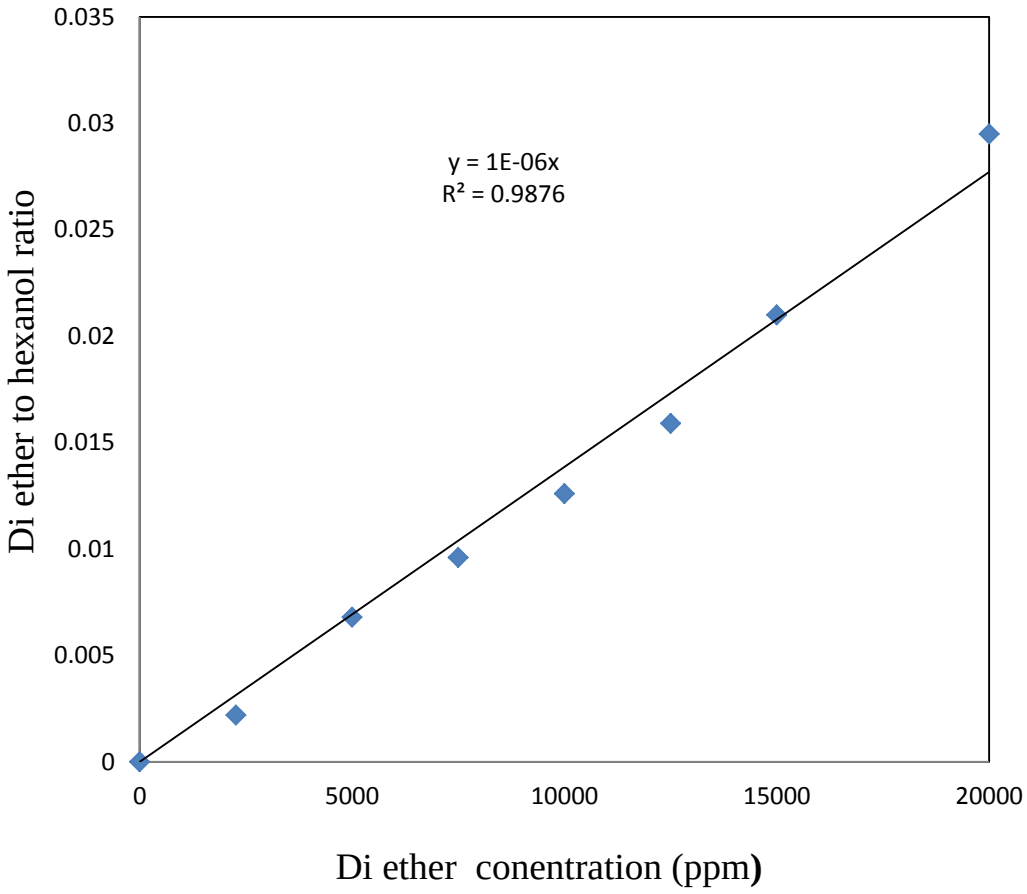

Figure E.2: Di tert-butyl glycerol ether calibration

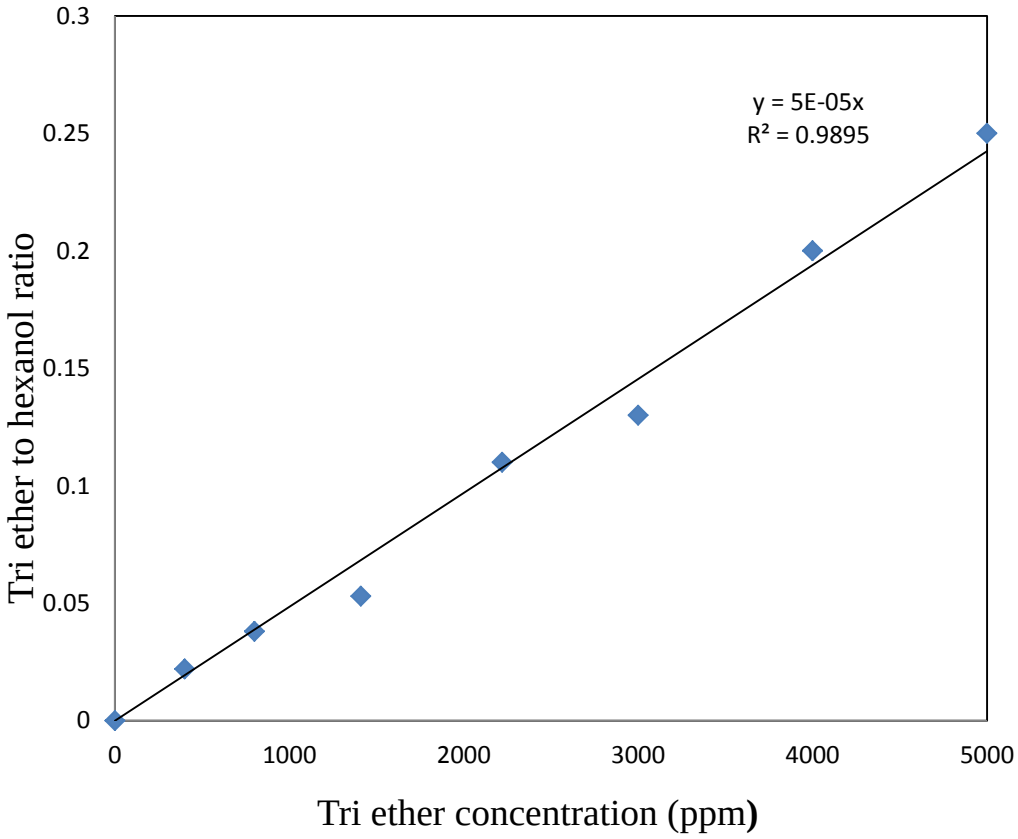

Figure E.3: Tri tert-butyl glycerol ether calibration